

The University of Akron IdeaExchange@UAKron

Honors Research Projects

The Dr. Gary B. and Pamela S. Williams Honors
College

Spring 2018

Sandia Senior Design Collaboration: Vacuum Sensor Design

James L. Valerio

The University of Akron, jlv50@zips.uakron.edu

Eric J. Black

The University of Akron, ejb63@zips.uakron.edu

Joseph P. Bednarz

The University of Akron, jpb74@zips.uakron.edu

David R. Warther

The University of Akron, drw69@zips.uakron.edu

Please take a moment to share how this work helps you [through this survey](#). Your feedback will be important as we plan further development of our repository.

Follow this and additional works at: http://ideaexchange.uakron.edu/honors_research_projects

 Part of the [Other Mechanical Engineering Commons](#)

Recommended Citation

Valerio, James L.; Black, Eric J.; Bednarz, Joseph P.; and Warther, David R., "Sandia Senior Design Collaboration: Vacuum Sensor Design" (2018). *Honors Research Projects*. 735.

http://ideaexchange.uakron.edu/honors_research_projects/735

This Honors Research Project is brought to you for free and open access by The Dr. Gary B. and Pamela S. Williams Honors College at IdeaExchange@UAKron, the institutional repository of The University of Akron in Akron, Ohio, USA. It has been accepted for inclusion in Honors Research Projects by an authorized administrator of IdeaExchange@UAKron. For more information, please contact mjon@uakron.edu, uapress@uakron.edu.

THE UNIVERSITY OF AKRON



Sandia Senior Design Collaboration

Vacuum Sensor Design

Mechanical Engineering - Spring 2018

Faculty Advisor:
Dr. D. Dane Quinn

Authors:
Eric Black
James Valerio
Joseph Bednarz
David Warther

Executive Summary

Sandia National Laboratories has requested a fully mechanical device to close a circuit after launch has occurred and the device enters a vacuum. Intended for applications in rockets and missiles, the device must fit in a 36 degree wedge with a 6.8 inch radius that is 6 inches in height and be ready to bolt onto a rocket. The pressure switch must be prevented from actuating until a launch acceleration ranging from 20 to 27g is detected. The pressure switch must close the circuit after a pressure of 10^{-1} Torr is reached and before a pressure of 10^{-6} Torr is reached. The switch must remain closed after the switch is actuated. The pressure switch is required to close a circuit carrying 30 VDC with a 15 ohm load for up to 15 seconds. The switch itself is allowed to have a maximum resistance of 0.2 ohms. The switch must be resettable for Sandia to conduct multiple test runs. Our contact at Sandia expressed interest in 3D printed components.

This design detects the launch acceleration by separating a calibrated mass from a magnet. Before the acceleration sensor is tripped, it prevents the pressure switch from actuating. The pressure switch contains a substance which is a liquid at the temperatures and pressures experienced before the vacuum environment is reached and vaporizes in the vacuum environment. The phase change causes an expansion of the fluid container, which is used to move the actuator magnet near a reed switch and close the circuit. Thus, this project applies thermodynamics, system dynamics, numerical methods, material selection, and mechanical component design.

A prototype of the design will be built and sent alongside a report to Sandia National Laboratories. Sandia will test the device on a sounding rocket. This project will provide Sandia with one of ten prototype devices to test. The switch provided will be used to detect when the rocket has left the atmosphere and has activated safety measures.

Acknowledgements

Our design group would like to thank the following individuals and organizations.

- Dr. D. Dane Quinn, University of Akron: Faculty Advisor
- Adam Brink, Sandia National Laboratories: Project Mentor at Sandia
- Steve Gerbitz, University of Akron: Machining calibrated masses
- FastForming, LLC, Rittman OH: Provided thermoforming services for FEP diaphragm
- American Durafilm, Holliston MA: Provided FEP film for thermoforming
- Additive Engineering Solutions, Akron: CNC machining of aluminum manifold
- William Wenzel, University of Akron: Finishing work on aluminum manifold
- Michael Weaver, University of Akron: 3D printing the base

Table of Contents

Executive Summary.....	1
Acknowledgements	2
Table of Figures.....	5
List of Tables	6
Table of Equations.....	6
Chapter 1: Introduction.....	7
1.1 Background	7
1.2 Principles of Operation	7
1.3 Product Definition.....	8
Chapter 2: Conceptual Design	9
2.1 Preliminary Design Brief	9
2.2 Expanded Design Brief	9
2.3 Function Structure Diagrams	9
2.4 Morphological Chart	11
2.5 Concept Sketches	11
2.6 Objective Tree.....	13
2.7 Weighted Decision Matrix	13
Chapter 3: Embodiment Design.....	15
3.1 Embodiment Rules	15
3.2 Embodiment Principles	15
3.3 Failure Mode and Effect Analysis.....	16
3.4 Preliminary Selection of Materials and Manufacturing Processes	16
3.5 Calculations.....	17
3.6 Layout Drawings.....	18
Chapter 4: Detail Design	19
4.1 Acceleration Switch Numerical Model	19
4.2 Analysis of Phase Change Fluids (PCFs).....	22
4.3 Standard Components List	23

4.4	Materials and Manufacturing Methods Selected.....	23
4.5	Bill of Materials and Cost Estimation	25
4.6	Test Procedures and Results.....	26
Chapter 5: Discussion.....		28
Chapter 6: Conclusions.....		31
References		32
Appendices		34
	Additional Figures	34
	Part Drawings	36
	Assembly Drawing	41
	Exploded View	42
	Matlab Scripts.....	44
	Magnet Data from K&J Magnetics With Curve Fit.....	46
	Vapor Pressure Plots.....	48
	Additional Concept Drawings.....	49

Table of Figures

Figure 1: Overall Function Structure Diagram	9
Figure 2: Detailed Function Structure Diagram.....	10
Figure 3: Morphological Chart	11
Figure 4: Concept sketches for concepts 1 - 6	13
Figure 5: Vacuum Sensor Objective Tree.....	13
Figure 6: Layout drawings with major dimensions	18
Figure 7: Free Body Diagram for acceleration switch mass	20
Figure 8: ODE15s Solutions for acceleration switch mass position and velocity with a rocket acceleration of 27g ..	21
Figure 9:ODE15s Solutions for acceleration switch mass position and velocity with a rocket acceleration of 15g ...	22
Figure 10: Density vs. Price per kg.....	34
Figure 11: Strength vs Density * Price	35
Figure 12: Al-Bronze slug Drawing	36
Figure 13: 3D printed base Drawing.....	37
Figure 14: Expanded PTFE Gasket Drawing.....	38
Figure 15: Pressure Sensor manifold Drawing	39
Figure 16: 3D printed top Drawing	40
Figure 17: Assembly Drawing.....	41
Figure 18: Exploded View Render	42
Figure 19: Vapor Pressure Plots	48
Figure 20: 3D Concept Drawing.....	49
Figure 21: Set and Unset Positions	50

List of Tables

Table 1: Weighted decision matrix with the chosen design highlighted.....	14
Table 2: Failure Mode and Effect Analysis	16
Table 3: Preliminary Material Choices	17
Table 4: List of Standard Components	23
Table 5: BOM and Cost Estimation.....	25
Table 6: Exploded View Component List	43

Table of Equations

Equation 1: Governing differential equation for accelerometer mass.....	20
Equation 2: Scaled curve fit for magnetic force	20
Equation 3: Contact Force	20
Equation 4: Smoothed, numerical rewriting of Equation 3	20

Chapter 1: Introduction

1.1 Background

Sandia National Laboratories has made a request to multiple universities, including the University of Akron, to create a prototype vacuum sensor. The vacuum sensor detects when a rocket has launched and exited the atmosphere. This is used to close a circuit which activates safety measures to prevent energy transfer through the rocket. The vacuum sensor will detect launch accelerations between 20 and 27g, and close a circuit when a pressure between 0.1 and 10^{-6} Torr is reached. The circuit must remain closed once the switch has been activated.

1.2 Principles of Operation

Outlined in Figure 6, the vacuum sensor has 3 main components, which are an acceleration switch, expanding diaphragm with a phase change fluid (PCF), and an electrical switch. The pressure switch's FEP diaphragm is blocked from expanding by a mass held in place by a magnet. When the launch accelerates the system above 20g, the mass separates from the magnet and falls into a channel. With the magnet in the channel, the diaphragm is free to expand. The diaphragm contains propylene glycol which exists in the liquid phase at the conditions which occur before the vacuum is reached. Once the pressure drops between 10^{-1} and 10^{-6} Torr, the propylene glycol will vaporize, expand the diaphragm, and close the circuit by moving an actuator magnet close to a reed switch. The reed switch is composed of two overlapping magnetic beams in a sealed glass tube. When the reed switch is placed in a sufficiently strong magnetic field, the beams will make contact and close the circuit. The overall system is designed to be bi-stable.

1.3 Product Definition

Our device is designed to close a circuit after a rocket has launched and exited the atmosphere. An acceleration switch consisting of a calibrated mass attached to a magnet is used to detect when the acceleration of the rocket exceeds 20g. A PCF in an expanding diaphragm is used to detect when the rocket is exposed to pressures between 0.1 and 10^{-6} Torr. To be mounted in the allotted rocket space the vacuum sensor must fit into a 36 degree wedge with a radius of 6.8 inches and a height of 6 inches. Our design seeks to accomplish these tasks in a simple manner with few moving parts to reduce to possible points of failure and increase reliability. Since this device is used as a safety measure reliability is a priority.

Chapter 2: Conceptual Design

2.1 Preliminary Design Brief

The goal of this project is to design a lightweight, resettable, and fully-mechanical pressure switch to activate in the range between 10^{-1} and 10^{-6} Torr. It must close a circuit with less than 0.2 ohm resistance. This switch must only be able to activate after a 20-27g acceleration.

2.2 Expanded Design Brief

Sandia National Labs requires a fully mechanical launch check system. The switching part of this system must only be able to activate after a 20-27g acceleration and at a pressure between 10^{-1} and 10^{-6} Torr. The activation is defined as the switching on of a current of 15 ohm with a potential of 30 VDC. This switching system must be able to actuate with bi-stability and then be reset manually for ease in testing the switch. The system also has to mount firmly in the space allotted in the rocket or missile. This space is defined by a 36 degree arc, a radius of 6.8 inches, and a height of 6 inches.

2.3 Function Structure Diagrams

Functionally, the vacuum sensor accepts launch acceleration and pressure conditions as inputs and then outputs a closed switch. The overall function structure diagram is shown in Figure 1. A more detailed view shows that the acceleration sensor/switch takes launch acceleration as an input. The outputs of the acceleration sub-function are energy and the removal of motion constraints on the pressure sensor. The damper converts the inertial energy from the acceleration switch to heat and work to ensure that the acceleration switch cannot return to its initial position. The now unconstrained pressure switch accepts pressures within the specified range as an input and outputs the closing of the circuit. The detailed function structure diagram is shown in Figure 2.

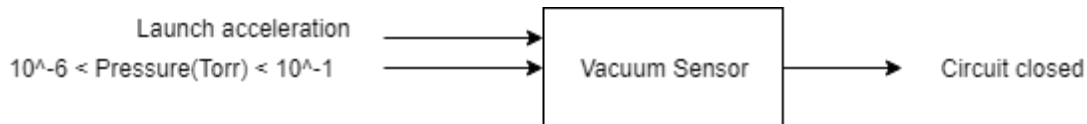


Figure 1: Overall Function Structure Diagram

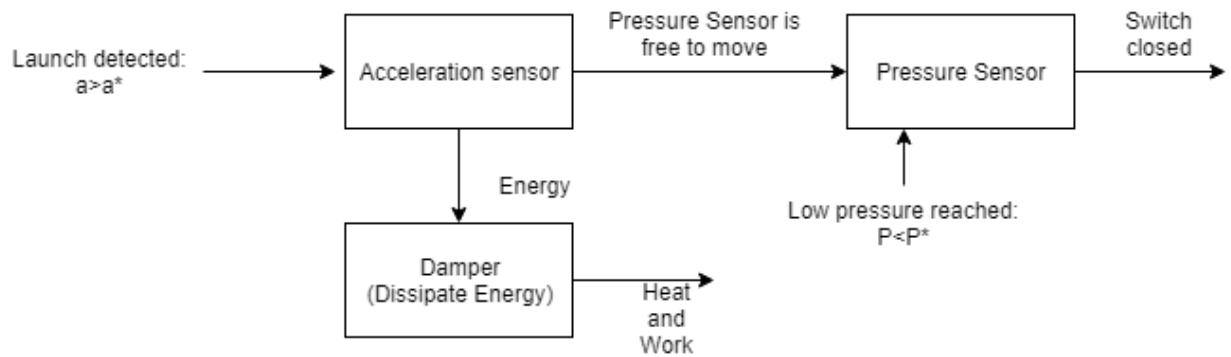


Figure 2: Detailed Function Structure Diagram

The detailed function structure diagram was used to layout the tasks which must be accomplished by the designed system. This information was used to brainstorm multiple methods to accomplish each task. These methods are shown in the morphological chart. Since Sandia requested a fully mechanical system, only methods that operate on mechanical methods were considered.

2.4 Morphological Chart

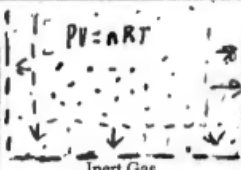
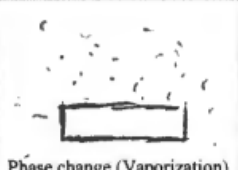
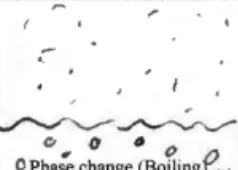
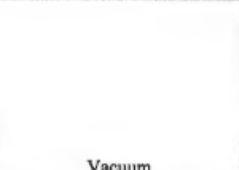
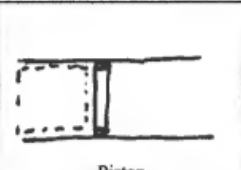
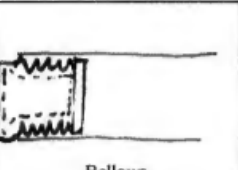
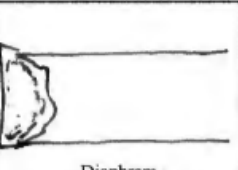
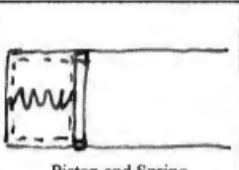
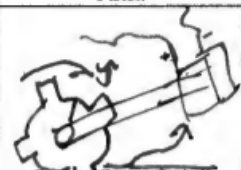
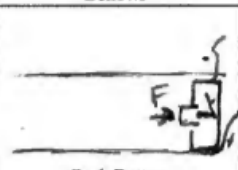
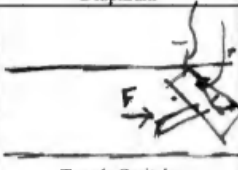
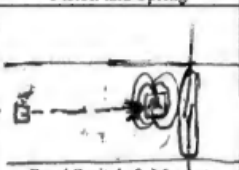
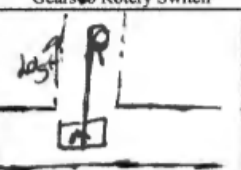
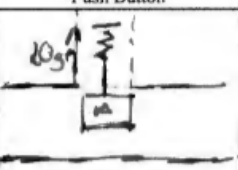


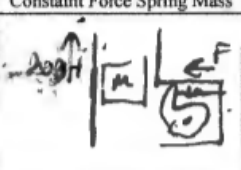
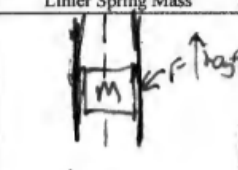


Morphological Chart for System				
Subsystem	Concepts			
Pressure Measurement Fluid	 Inert Gas	 Phase change (Vaporization)	 Phase change (Boiling)	 Vacuum
Fluid Containment	 Piston	 Bellows	 Diaphragm	 Piston and Spring
Switching Mechanism	 Gears Rotary Switch	 Push Button	 Toggle Switch	 Reed Switch & Magnet
Acceleration Verification	 Constant Force Spring Mass	 Linear Spring Mass	 Replaceable Spring Mass	 Magnet and Mass
Accelerometer Stop and damping	 Mass Lock (sprocket)	 Friction	 Friction and Foam Stop	 Grease

Figure 3: Morphological Chart

2.5 Concept Sketches

From the morphological chart, 6 concepts were created. Sketches of each concept are shown in Figure 4.

Concept 1 uses a spring mass system to detect launch acceleration. As the mass moves into the tripped position a locking device snaps into place keeping the mass in its switched position. When the external pressure drops, the differential pressure between the interior and exterior of the inert gas reservoir will cause the gas in the reservoir to expand and move a toothed piston.

The piston motion will transfer through a set of gears to drive the rotation of a rotary switch and close the circuit.

Concept 2 uses the same pressure and acceleration sensing methods as concept 1, but the pressure difference is used to push the piston into a push button switch and close the circuit. Locking mechanisms snap into place to keep the piston in its final position with the circuit closed.

Concept 3 uses a mass attached to a magnet to detect acceleration. When launch is detected, the magnet falls into a channel. Since magnitude of the magnetic field approaches zero as the mass moves away from the magnet, no locking mechanism is required to prevent the magnet from pulling the mass back. When a low pressure is reached, the inert gas will expand as in concept 1, and the expansion of the bellows moves a magnet toward a reed switch. The reed switch closes the circuit in the presence of the magnetic field. Retaining magnets are placed near the end of the expansion shaft to hold the actuator magnet in its final position.

Concept 4 uses the locking mass spring system to detect acceleration. A PCF vaporizes and expands a diaphragm with a rigid plate attached. To ensure this, a fluid with a vapor pressure in the desired pressure range is selected. The expansion will press the plate against a toggle switch and force it into the closed position. No retaining methods are required for the expanding portion since the toggle switch will remain closed once it is switched.

Concept 5 uses the magnet and mass acceleration sensor and an inert gas to expand the piston. The piston motion pushes the toggle switch into the closed position.

Concept 6 uses the magnet and mass acceleration sensor and the PCF to detect pressures. The diaphragm has an actuator magnet attached and its expansion moves the magnet within range of the reed switch.

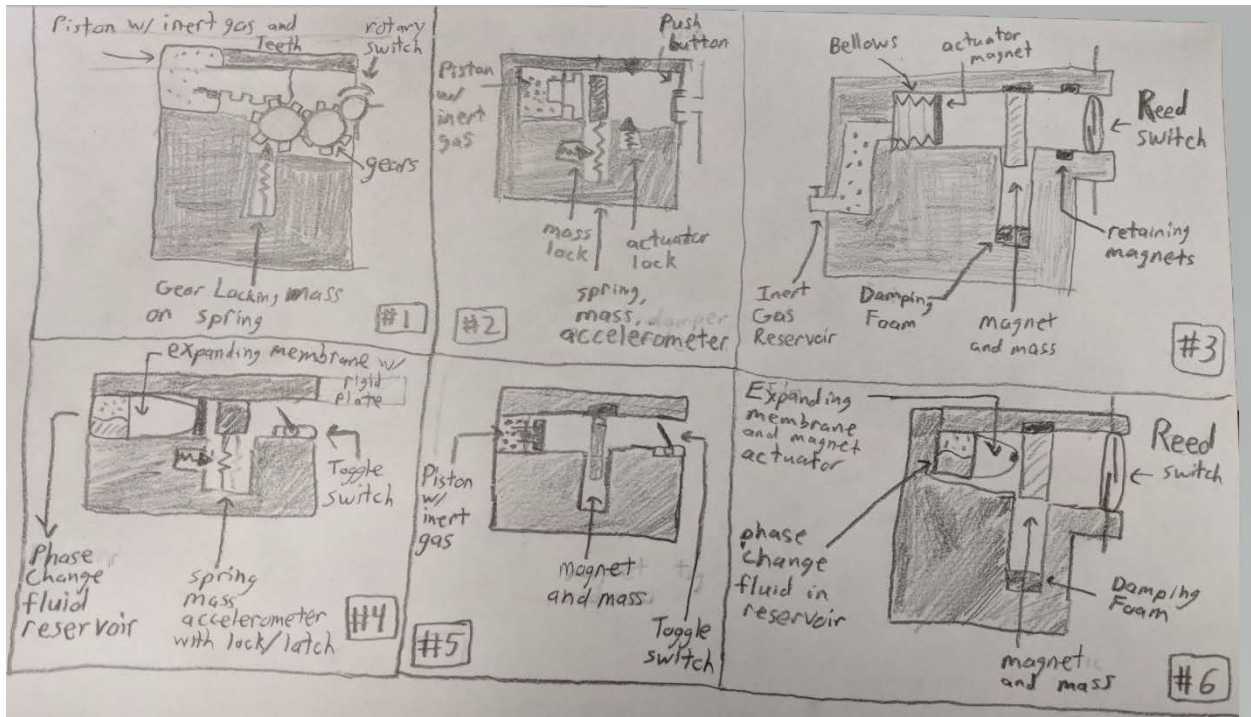


Figure 4: Concept sketches for concepts 1 - 6

2.6 Objective Tree

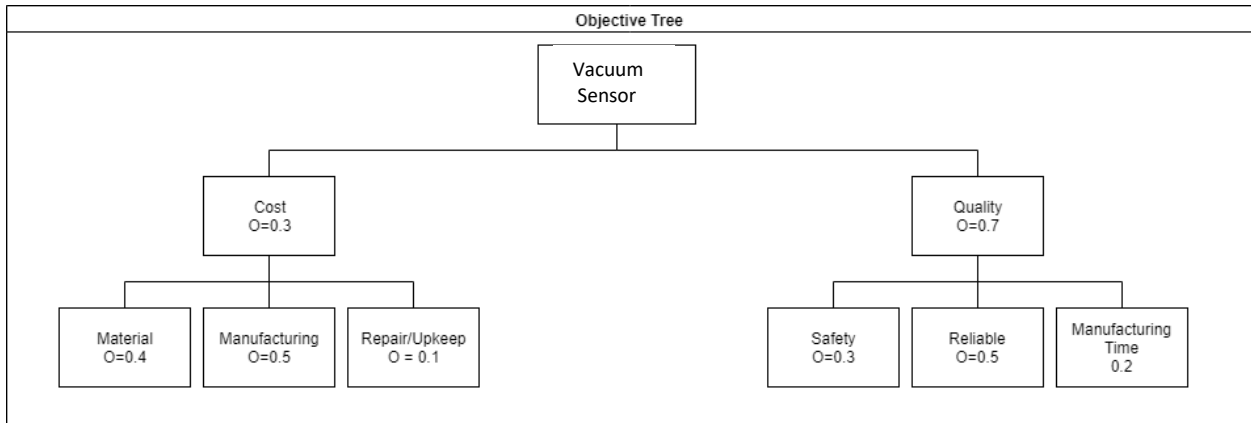


Figure 5: Vacuum Sensor Objective Tree

2.7 Weighted Decision Matrix

The weighted decision matrix shown in Table 1 is populated with weight factors determined from the objective tree. Each design is given a score in each design criteria which is multiplied by the weight factor. The scores for each design are summed and the design with the highest score is chosen. Concept 6 had the highest score.

Due to the similarities in device sizes and possible material choices, the material cost score for each concept was the same. The manufacturing costs of the designs involving gears or bellows were given poor manufacturing cost scores due the high cost of custom sized gears, complexity of machining small precise components, and the complex manufacturing process for bellows. A poor repair cost was given to the bellows and gear based designs, since replacement gears or bellows would have a high cost. All concepts were given high safety ratings since each one has moving parts enclosed and any potentially hazardous substances are sealed within a reservoir. Concepts 4 and 6 received the highest reliability scores because they contain the fewest number of moving parts. Designs with gears or spring loaded locking mechanisms received low scores due to a greater number of moving parts, which may fail. Concepts 1 and 3 received low scores for manufacturing time due to the complexity of manufacturing bellows and small precise gears and applying teeth to the piston that can mesh with the gears.

Table 1: Weighted decision matrix with the chosen design highlighted

		CONCEPT #											
		1		2		3		4		5		6	
Design Criteria	Weight Factor	Score	Rating	Score	Rating	Score	Rating	Score	Rating	Score	Rating	Score	Rating
MATERIAL COST	0.12	7	0.84	7	0.84	7	0.84	7	0.84	7	0.84	7	0.84
MFG COST	0.15	3	0.45	4	0.6	1	0.15	4	0.6	5	0.75	8	1.2
REPAIR COST	0.03	3	0.09	5	0.15	1	0.03	6	0.18	5	0.15	8	0.24
SAFETY	0.21	9	1.89	9	1.89	9	1.89	9	1.89	9	1.89	9	1.89
RELIABILITY	0.35	4	1.4	5	1.75	7	2.45	4	1.4	5	1.75	8	2.8
MFG TIME	0.14	2	0.28	7	0.98	2	0.28	7	0.98	7	0.98	7	0.98
TOTAL SCORE			4.95		6.21		5.64		5.89		6.36		7.95

Chapter 3: Embodiment Design

3.1 Embodiment Rules

The embodiment design maintains clarity of function, simplicity, safety, and reliability. The reed switch, acceleration switch, and pressure sensor each carry out one function uncoupled from other functions. The components are arranged such that both the acceleration switch and pressure sensor must be activated to close the electrical connection. The design maintains simplicity by reducing the number of moving parts to a few essential components. Simplicity reduces probability for unexpected behavior during use and makes the design more reliable. The calibrated mass falls into a channel at a calculated acceleration. The PCF expands at a given temperature and pressure. By limiting the number of steps and moving parts between the sensors and the switch, reliability is improved. Safety is insured by containing moving parts within a housing and using safe PCFs.

3.2 Embodiment Principles

The first principle observed is self-help. Once the PCF is able to vaporize, the small magnet in the diaphragm can move farther from the centerline of the sounding rocket. This movement away from the center line increases the centripetal force on the magnet and helps the pressure sensor expand. This is important because during vaporization at such low pressures, the work done by the expanding gas is small. Division of tasks is the next principle observed. Each component has a specialized purpose and task. The last principle used is stability. The acceleration switch operates as a bi-stable system. Once the mass separates from the magnet, the system must stabilize in its new state. The acceleration of the rocket keeps the magnet in this state. To prevent any bounce-back, foam is inserted into the hole so that energy is absorbed.

3.3 Failure Mode and Effect Analysis

Table 2 below shows how the vacuum sensor could fail and the severity of each failure.

Table 2: Failure Mode and Effect Analysis

Component	Potential Failure Mode	Potential Effect(s) of Failure	Severity	Potential Cause(s)/ Mechanism(s) of Failure	Current Process Controls
Acceleration switch	Calibrated mass does not separate from magnet	The pressure switch cannot operate	10	Improper size hardware	Test separation force
	Mass bounces up after separation	The pressure switch cannot operate	9	Insufficient energy absorption	Check that foam is in place
Pressure Switch	Leak in diaphragm	Pressure sensor cannot expand	10	Improper Handling	Check before installing fluid
	Leak in gasket	Loss of PCF	8	Insufficient gasket seating	Check before installing fluid
	Freezing PCF	Change vapor pressure	7	Temperature change, latent heat of vaporization	Insulate switch
	Fluid cannot constrain magnet	Early electrical connection	7	Diaphragm too loose	Pull on magnet
Reed Switch	Stuck switch	No electrical connection	8	Faulty reed switch	Test switches before insulation
	Cracked glass	Function improperly	6	Damaged reed switch	Visually inspect switch

3.4 Preliminary Selection of Materials and Manufacturing Processes

Materials were selected for this design based on minimizing mass and cost, while still meeting the requirements of each component. The material list for the entire system was filtered by seeking materials that can operate between -90 and 90°C. The acceleration switch mass must be small, but heavy enough to separate from the magnet during launch. To achieve the desired mass in the available volume, a high density is required. Additionally mass materials were limited to nonferrous metals and plastics. Figure 10 plots material density versus cost per unit mass using CES EduPack 2018 (Granta Design Limited, 2017). The mass will have a steel insert to allow it to stick to the acceleration switch magnet, but not interfere with the magnets used to activate the reed switch. The PCF reservoir must be chemical resistant and non – porous. The

expandable diaphragm must be a thin film, chemical resistant, low outgassing, and formable into the desired shape. The base must be nonmagnetic, and a material with low electrical conductivity is desirable. Acceptable material choices are summarized in Table 3 below.

Table 3: Preliminary Material Choices

Component	Desired Properties	Acceptable Materials
Acceleration switch mass	Inexpensive, Dense, Non-magnetic	Stainless Steels, Aluminum Bronzes, Brass, Lead
Fluid Reservoir	Chemical resistant, non-porous	Aluminum alloys, Brass, PTFE
Expandable Diaphragm	Chemical resistant, Formable, low outgassing	FEP, PFA, Kapton
Base	Inexpensive, lightweight, nonmagnetic	Polycarbonate, Aluminum Alloys, Brass, PTFE, Polypropylene

Based on the preliminary material selections, possible manufacturing techniques were determined. The acceleration switch mass will be machined. The fluid reservoir must be machined or injection molded. The expandable diaphragm will require thermoforming or heat sealing. The base can be injection molded, machined, or 3D printed.

3.5 Calculations

A switch capable of handling the required loads is needed. The switch data sheets give a switching voltage, power, and current. Given the DC voltage and resistance, the switching current and power is calculated below.

$$V = 30 \text{ VDC} \quad R = 15\Omega$$

$$I = \frac{V}{R} = \frac{30V}{15\Omega} = 2A$$

$$P = VI = 30V * 2A = \mathbf{60W}$$

As the rocket flies, it rotates about the center of top cross section at a frequency of 4 Hz. This rotation will apply centripetal acceleration to the internal components. Given the spin rate, and maximum radial location of the vacuum switch, the maximum expected centripetal acceleration is calculated below.

$$f = 4\text{Hz}, \quad \omega = 2\pi f = 8\pi \frac{\text{rad}}{\text{s}}, \quad r = 6.8\text{in} = 0.567\text{ft}$$

$$a_c = r\omega^2 = 0.567\text{ft} \left(8\pi \frac{\text{rad}}{\text{s}}\right)^2 = \mathbf{358 \frac{ft}{s^2}}$$

3.6 Layout Drawings

The vacuum sensor is arranged such that the accelerometer shaft is parallel to the direction of the rockets motion. This ensures that the acceleration switch detects the launch acceleration. The reservoir is connected to the base with screws or bolts, and arranged such that the diaphragm expands outward from the center of the rocket. This ensures that the centripetal acceleration due to the rocket spin rate assists the diaphragm in moving the switch actuating magnet instead of opposing it.

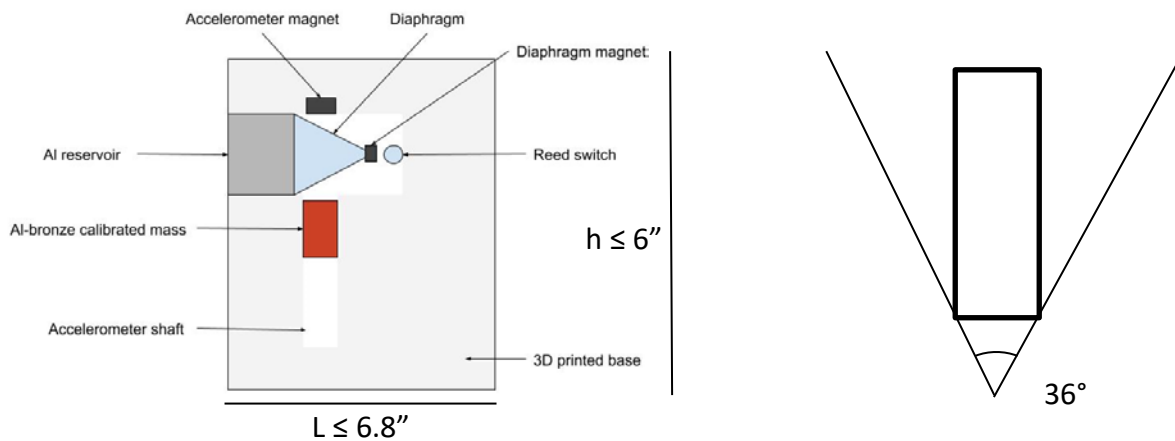


Figure 6: Layout drawings with major dimensions

Chapter 4: Detail Design

4.1 Acceleration Switch Numerical Model

The free body diagram for the acceleration switch is shown in Figure 7. The acceleration switch mass travels through a channel which restricts motion along all other axes. This allows us to simplify the acceleration switch to a one degree of freedom model. The mass is connected to the rocket by magnet. A contact force F_c must be applied before the mass and magnet will separate. The governing differential equation for this system is given by Equation 1.

A function for the magnetic force F_m was determined using test data from the K&J Magnetics webpage for the specified magnet. Data was generated in laboratory conditions by measuring the force required to pull the magnet from a smooth, thick steel plate, so the listed forces are expected to be higher than those observed in application (K&J Magnetics). The distance from the magnet where 0.75 lbf of pull force occurred was determined experimentally; this occurred between 0.010 and 0.015 inches from the magnet surface. A curve of the form Ae^{Bx} was fit to the data and scaled such that the pull force of 0.75 lbf occurred at the experimentally determined distance of 0.0125 inches. The function was offset such that $x = 0$ occurs 0.015 inches from the magnet surface. Equation 2 gives the scaled curve fit for the magnetic force, F_m as a function of distance, x in feet. The contact force, F_c is defined by Equation 3.

Due to the nonlinearity of the governing differential equation, the solution is found numerically. Numerical methods behave irregularly when given sharp jumps as seen in F_c , or other functions like the unit step and Dirac-delta functions. Equation 3 was smoothed and rewritten as Equation 4 to avoid this issue by assuming that F_c behaved as a stiff spring for all x less than a small positive value. This assumption is based on the fact that materials are typically not rigid and it is possible for small deformations in the magnet or mass allowing the x position to be defined for some negative x . Due to the sharp jump in the contact force function and an anticipated sharp jump in the solution we consider this to be a stiff problem. Equation 1 input into the Matlab ODE solver ODE15s to estimate the position and velocity of the acceleration switch mass along the x -coordinate. ODE15s was used due to Mathwork's claim that ODE15s shows the greatest performance for most stiff problems (Mathworks, 2018).

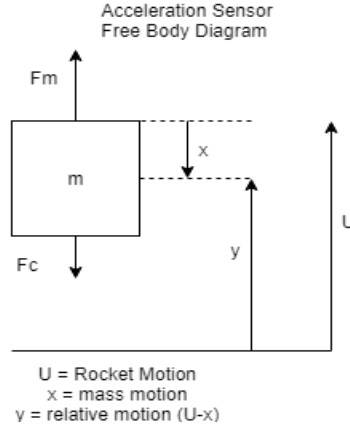


Figure 7: Free Body Diagram for acceleration switch mass

$$m\ddot{x} - F_m(x) - F_c = ma_{rocket}$$

Equation 1: Governing differential equation for accelerometer mass

$$F_m \approx 0.942e^{-238(x+0.00125)} lbf$$

Equation 2: Scaled curve fit for magnetic force

$$F_c(x) = \begin{cases} F_m(0) - ma_{rocket} & \text{if } x = 0 \\ 0 & \text{if } x > 0 \end{cases} lbf$$

Equation 3: Contact Force

$$F_c(x) = \begin{cases} 10^6(F_m(0) - ma_{rocket})x + (F_m(0) - ma_{rocket}) & \text{if } x < 10^{-6} ft \\ 0 & \text{if } x > 0 \end{cases} lbf$$

Equation 4: Smoothed, numerical rewriting of Equation 3

The solution shows the mass remaining stationary when the rocket is not accelerating. When the acceleration is below 20g the mass initially oscillates with small displacements that quickly decay to even smaller oscillations. These small oscillations continue as time passes without dissipating since there is no damping term in the model. The magnitude of these oscillations is small enough to be considered negligible. Thus, the mass does not leave its starting state and continues restricting possible expansion of the diaphragm. This is shown in Figure 9. When the rocket's acceleration exceeds 20g, the mass pulls away from the magnet and the displacement increases rapidly. Based on the design the acceleration switch mass will collide with the end of the channel built into the base when $x = 4$ inches. Unless sufficient energy is dissipated, the mass will bounce back up into its original position. To create a bi-stable system, a

1 inch tall open cell, polyurethane foam piece was placed into the channel. When struck by the mass, the foam piece will compress and buckle. The buckling of the foam cells and structure dissipates some of the energy from the acceleration switch mass (Hillyard & Cunningham, 1994). Since the mass will impact the foam at $x = 3$ inches, the energy in the acceleration switch mass at $x = 3$ inches is of interest. The maximum energy in the mass for this application will occur for the largest possible acceleration in the launch profile at 27g. The numerical solution shows that the mass is displaced 3 inches after 0.026 seconds with a velocity of 20.1 feet per second. This is shown in Figure 8. The total energy available in the mass is calculated below. The expected mass determined from the CAD model is used below.

$$m = 0.035\text{lbm} = 1.1 * 10^{-3}\text{slug} \quad g = 27 * \frac{32.2\text{ft}}{\text{s}^2} = 869.4 \frac{\text{ft}}{\text{s}^2} \quad h = 1\text{in} = 0.083\text{ft}$$

$$V = 20.1 \text{ ft/s}$$

$$E = \frac{1}{2}mV^2 + mgh$$

$$= \frac{1}{2}1.1 * 10^{-3}\text{slug} \left(20.1 \frac{\text{ft}}{\text{s}}\right)^2 + 1.1 * 10^{-3}\text{slug} \left(869.4 \frac{\text{ft}}{\text{s}^2}\right)(0.083\text{ft}) = 0.302 \text{ lbf} * \text{ft}$$

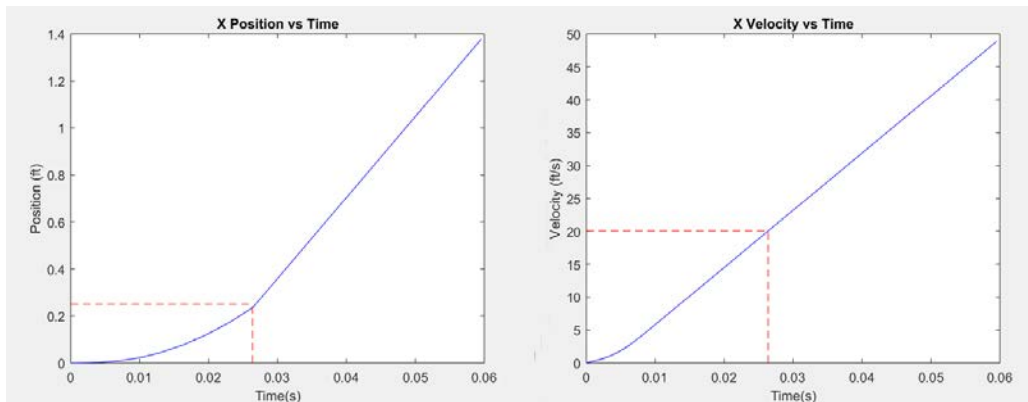


Figure 8: ODE15s Solutions for acceleration switch mass position and velocity with a rocket acceleration of 27g

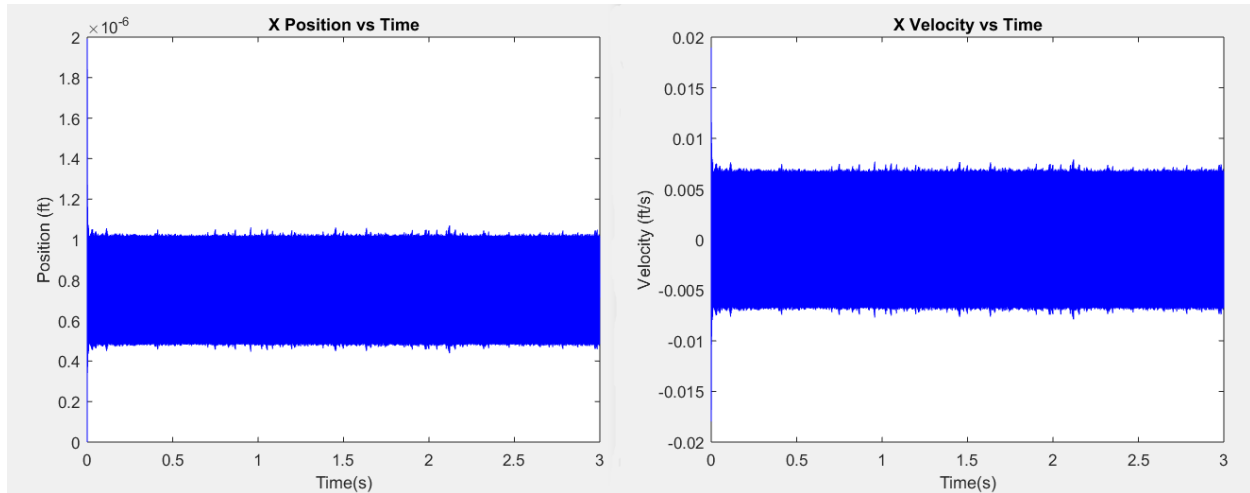


Figure 9:ODE15s Solutions for acceleration switch mass position and velocity with a rocket acceleration of 15g

4.2 Analysis of Phase Change Fluids (PCFs)

A variety of potential PCFs were analyzed by plotting their vapor pressures across a range of temperatures. The temperature and pressure expected along the rockets path is also plotted. Plausible substances were identified by observing an intersection of the rocket conditions and the vapor pressure curve in the desire pressure range. The selected fluid was propylene glycol. This decision is discussed further in Chapter 5.

4.3 Standard Components List

Table 4: List of Standard Components

Part Name	Catalogue	Part Number
N52 Neodymium Ring Magnet, 1/16” ID, 1/8” OD, 1/16” Height	K&J Magnetics	211-N52
N 42 Neodymium Ring Magnet with #4 Countersunk Hole	K&J Magnetics	R622CS-P
Littlefuse Reed Switch 3A 400VDC 100VA *	Arrow Electronics	D6-129-47-68 *
10 – 32 screw	McMaster Carr	91321A127
10 – 32 wing nut	McMaster Carr	98671A190
6-32 SS socket head cap screw	McMaster Carr	92200A146
1/8 NPT PTFE plug	McMaster Carr	45375K252
4-40 SS flat head screw	McMaster Carr	92805A108

* Note: The Littlefuse D6-129-47-68 is obsolete and will be replaced by the Littlefuse DRS-50-47-68. This component will be available as of May 31st, 2018.

4.4 Materials and Manufacturing Methods Selected

The material selected for the PCF reservoir/manifold and flange was 6061 aluminum alloy. This material was chosen for its low density, ability to be used in the working temperatures seen by this device, and its good corrosion resistance rating to ethylene glycol and propylene glycol (CP Lab Safety, 2018). 6061 aluminum was selected over other aluminum alloys due to its lower cost and availability. These components were CNC machined to get the correct geometry with the necessary holes. After machining, threads were tapped into holes where fasteners will be applied. The expanding diaphragm was constructed from 0.020 inch thick FEP film. This material was selected for its excellent resistance to a variety of chemicals, nonstick properties, and ability to be formed into the desired shape (ThermoFischer Scientific). Additionally, the FEP film meets NASA low outgassing standards. The FEP film was cheaper and more easily available in a variety of thicknesses than the PFA or Kapton films. The FEP diaphragm was thermoformed into the desired shape. The acceleration switch mass sleeve was made from 954 bearing bronze (Aluminum Bronze). This material was selected due to its high density and

middle range cost. An alternative option would be AISI 205 Stainless Steel, which has a similar density at a much lower cost (Granta Design Limited, 2017). The aluminum bronze was selected over the stainless steel due to its superior friction and wear properties. These properties were valued since the mass will be sliding through a channel when the switch trips. The mass was machined from 0.5 inch diameter rod on a lathe. Polycarbonate was selected to be the material for the base. Polycarbonate was chosen due to its ability to be 3D printed, ability to withstand our applications working temperatures, low density, and higher strength than other available thermoplastics like polypropylene (Granta Design Limited, 2017). The base was 3D printed due to our contact at Sandia expressing interest in 3D printable components. Additionally, 3D printing provides quick prototyping and the ability to manufacture complex geometries.

4.5 Bill of Materials and Cost Estimation

Table 5: BOM and Cost Estimation

Part #	Part Name	Description	Qty	Units	Unit Cost	Cost
1	Calibrated Mass	used in accelerometer	N/A	each	N/A	
1.1	91321A127	10-32 screw	1	each	\$ 0.25	\$ 0.25
1.2	98671A190	10-32 wing nut	1	each	\$ 1.00	\$ 1.00
1.3	Al/Bronze Slug	custom made mass	1	each	\$ 165.22	\$ 165.22
2	Base	3D printed base fixture	1	each	\$ 183.19	\$ 183.19
3	Reed Switch	magnetic circuit closure	1	each	\$ 3.42	\$ 3.42
4	Top	3D printed top fixture	1	each	\$ 43.35	\$ 43.35
5	Pressure Sensor	pressure sensor	N/A	each	N/A	
5.1	Manifold	contains phase-change fluid	1	each	\$ 115.07	\$ 115.07
5.2	Gasket	Expanded PTFE gasket	2	each	\$ 2.00	\$ 4.00
5.3	FEP Expanding Membrane	allows phase-change fluid to expand	1	each	\$ 110.11	\$ 110.11
5.4	92200A146	6-32 SS socket head cap screw	4	each	\$ 0.36	\$ 1.43
5.5	45375K252	1/8 NPT PTFE plug	1	each	\$ 20.11	\$ 20.11
6	Accelerometer Magnet	magnet to hold calibrated mass	1	each	\$ 1.17	\$ 1.17
7	92805A108	4-40 SS flat head screw	5	each	\$ 0.24	\$ 1.20
8	Carbon fiber rod	allows actuator swing to pivot	1	each	\$ 5.00	\$ 5.00
9	Actuator swing	activates Reed switch with force from pressure sensor	N/A	each	N/A	
9.1	Wire loop	guides magnets in arc	1	each	\$ 1.00	\$ 1.00
9.2	N52 Ring Magnet	radial magnet used to actuate Reed switch	5	each	\$ 1.40	\$ 7.00
9.3	PTFE Wire Sleeve	attaches wire loop to carbon fiber rod	2	each	\$ 2.00	\$ 4.00
10	Rubber Damper	prevents calibrated mass from rebounding on launch	1	each	\$ 5.00	\$ 5.00
Total			31			\$ 671.51

4.6 Test Procedures and Results

The full system will be tested on a sounding rocket launch in summer 2018. Sandia National Laboratories will be conducting this test. To validate the proposed design, component level testing was performed.

The acceleration switch was designed to trip at an acceleration of 20g. The magnetic force required to hold the mass at this acceleration was found to be 0.75 lbf. The offset between the magnet surface and the accelerating mass was determined to be 0.015 inches. This was found by testing with both centrifugal and static loading. For the static load test, a 0.75 lbf test mass was hung from the magnet with shims between the magnet and test mass. The offset was determined by removing shims, allowing the mass to get closer to the magnet and experience greater pull force until the test mass was held above ground by the magnet. The 0.015 inch offset allowed the magnet to hold the test mass where even a small disturbance like blowing on the mass surface would cause the test mass and magnet to separate. For the centrifugal test, the switch mass and magnet were attached to a rotating arm such that the center of mass of the switch mass was 5.44 inches from the rotational axis of the centrifuge. The arm was rotated at angular velocities ranging from 0 to 360 rpm. This subjected the switch mass to accelerations from 0 to 20g, and the switch mass did not separate until the 20g acceleration was reached. The expected offset required to see 0.75 lbf of magnetic force was 0.0625 inches based on test data (K&J Magnetics). The data was acquired in lab conditions with the magnet attaching to a flat, thick steel plate. According to K&J Magnetics, the actual magnet force experienced will be lower than their test values due to imperfect surfaces, surface coatings, and inadequate thickness of the steel component. The data from K&J Magnetics is listed in the appendices.

The vacuum oven available was unable to reach a low enough pressure to vaporize propylene glycol. However, the device was filled with propylene glycol and sealed while submerged. The system was then placed in the vacuum oven to confirm that it would not expand early. For this run, the diaphragm expanded due to an air bubble in the system. A second filling was performed. This time, the diaphragm was submerged unsealed in propylene glycol and placed in the vacuum. The vacuum oven was run to pull any air out of the system. The device was removed from the vacuum and sealed, while still submerged. Then the sealed system was cleaned off and placed in the vacuum oven. The device still expanded in this run, but to a lesser

amount as the system still had air in it, but this amount was much smaller. Next, water was used to prove the concept of expanding the diaphragm with a liquid to vapor phase change. The reservoir and diaphragm were connected and submerged in water. The submerged component was placed in the vacuum to ensure no air was in the system. When the vacuum reached its lowest pressure the tap water outside the device began to boil and vaporize. The component was removed from the vacuum and sealed with the diaphragm pressed in while still submerged. Then, the system was placed in the vacuum oven at a temperature of 23°C. The pressure in the oven was reduced from atmospheric pressure to its lowest pressure. When the vacuum oven reached this pressure, the water began to vaporize and the vapor expanded the diaphragm as expected.

The number of magnets used in the actuator swing was determined experimentally. The system was assembled without the reservoir. The actuator swing started with one magnet and was moved from its starting position to its final position where the reed switch should close. One magnet was unable to close the switch. The test proceeded adding one more magnet to the actuator swing until the moving the actuator swing to its final position closed the switch every time. This occurred when 5 magnets were attached to the actuator swing. The magnets used are Grade N52 neodymium rings with a 0.0625 inch ID, 0.125 inch OD, and 0.0625 inch height.

Chapter 5: Discussion

The design requirements for a switch capable of carrying the specified load were met by selecting an off the shelf reed switch rated for the switching voltage, current, and power. The selected reed switch is manufactured by Littlefuse, has a maximum resistance of 0.1 ohm. Additionally, the switch is rated to operate under vibrations up to 30g and shock up to 100g (Littlefuse). Testing verified that our magnetic actuator could consistently close the reed switch when the magnets were placed within 0.125 inches of the switch. A magnet inside of the inflatable diaphragm restricts the motion of magnets to the outside surface of the diaphragm. When the PCF exists as a liquid, the magnets are constrained and cannot close the reed switch. When the PCF exists as a liquid-vapor mixture, the magnets are free to move towards the reed switch. Movement is assisted by centripetal acceleration. The magnets are supported by a wire in the vertical direction. If the pressure increases and the PCF condenses into a liquid, the magnets on the outside of the inflatable diaphragm cling to the reed switch, keeping the contacts closed.

The acceleration switch is shown in both a numerical model and from test results to separate from the magnet when a 20g acceleration is applied. The model was simplified to a one degree of freedom system and a numerical solution was found as discussed in the acceleration switch analysis section of Chapter 4. A foam piece was placed into the channel to dissipate energy from the falling mass to ensure that the acceleration switch mass did not bounce back up to its original position and reconnect to the magnet. Similar designs are used by Aerocon in their acceleration switches. Aerocon uses a specified mass placed in a container that drops from its open position when a given acceleration is applied along the axis where the switch allows motion (Aerocon, 2017).

Pressure dependent changes in vapor pressure are considered as a means of sensing pressure. The change between a state above the vapor pressure and below the vapor pressure is dramatic and observable. The phenomenon is also less susceptible to vibration than mechanical methods discussed previously. Vapor pressure is temperature dependent, therefore temperature must be controlled.

Cajori describes a method of measuring the vapor pressure of water and comparing vapor pressure data and pressure-altitude data to estimate altitude (Cajori, 1929). Pressure is held constant and water temperature is increased until boiling is observed. On mountains, this

thermometric method yielded results similar to triangulation, with errors typically less than 3%. 19th century physicists recognized the pressure dependent relationship of vapor pressure. The pressure switch operates on a similar principle. In the pressure switch, temperature is held constant and pressure decreases until it drops below the vapor pressure and the liquid begins to boil. A fluid can be chosen such that it exists as a vapor during the desired conditions. This fluid is referred to as the phase change fluid (PCF). Huo et al. also discuss a pressure sensor which operates by expanding a membrane by heating water until it vaporizes (Huo, Chuai, Yin, Liu, & Wang, 2006).

The required pressure range is provided in the requirements of the project. The PCF must exist as a vapor between 10^{-1} Torr and 10^{-6} Torr. According to a standard atmosphere, these pressures are expected at altitudes between 65 km and 280 km respectively (Lewis, 2007).

A temperature range is needed to select the PCF. A temperature profile within the rocket was not provided, so temperature range used to select the PCF is assumed. The PCF is in an insulated reservoir and surrounded by an insulating 3D printed base. The air inside the rocket at the beginning of the flight escapes. This reduces heat transfer from the fluid to the surrounding air. The pressure switch is assumed to be isolated from heat produced by the propulsion system. Therefore, no significant heat flux is expected into or out of the PCF. Latent heat of vaporization may reduce the temperature of the PCF during the phase change event. Considering the volume of the expanding diaphragm and treating the PCF as an ideal gas, a small amount of energy is required for the phase change. The aluminum manifold reheats the PCF close to the original temperature. By assuming the PCF temperature does not vary significantly during flight. A temperature range is chosen between 0°C to 21°C . This covers a range of possible launch site temperatures. A wider temperature range is desirable.

Potential PCFs are screened using vapor pressure data found on ChERIC and NIST websites. The PCF chosen must exist as a vapor between 10^{-1} Torr and 10^{-6} Torr within the temperature range of 0°C and 21°C . Potential PCFs include nonane, monoethylene glycol, diethylene glycol, and propylene glycol. Propylene glycol is selected because it has a low freezing point and is less hazardous than other potential fluids (Center for Disease Control, 1997). Vapor pressure plots are included in the appendices.

The PCF is contained within an inflatable fluorinated ethylene propylene (FEP) diaphragm. The diaphragm is connected to the reservoir with a flange and expanded PTFE gaskets to provide a gas tight seal. The reservoir's fill port is sealed with a PTFE plug with PTFE gas tape applied to the threads. When the vapor pressure is reached, the PCF becomes a vapor and the diaphragm inflates. Work is required to unfold the FEP diaphragm. Work due to differential pressure between the inside of the diaphragm and the environment is small. The expansion is assisted by centripetal acceleration due to the rotation of the rocket. Testing of the reservoir and FEP diaphragm system revealed that the method used to fill and seal the system allowed for the possibility of air pockets to remain trapped in the system and cause expansion before the desired pressure range is reached. A more robust potential alternative is proposed. The reservoir may be connected to a multi-port valve. One port will connect a vacuum pump to the reservoir and the other will connect the reservoir to a container of the PCF. These will further be referred to as port 1 and port 2 respectively. First, port 1 will be open and port 2 will be closed. The vacuum pump will be turned on to remove air from the reservoir diaphragm system. Once the air has been evacuated, port 2 will be opened to pull the PCF into the reservoir. Then, both ports will be closed, the vacuum pump turned off, and both connections removed. This will leave a sealed reservoir containing sufficient PCF and no air pockets.

Chapter 6: Conclusions

This vacuum sensor was designed to provide Sandia National Labs with a fully mechanical switch prototype capable of detecting launch acceleration and closing a circuit when the pressure falls within the 10^{-1} to 10^{-6} Torr range. The device was designed to fit within the specified footprint and be resettable for testing purposes. This design focused on increasing reliability by using minimal moving parts and simple methods to accomplish each task.

Testing and numerical solutions showed that the acceleration switch should trip and allow the diaphragm to expand when the desired pressure range is reached. The off the shelf reed switch meets the specified requirements and the actuator magnets are capable of providing a sufficient magnetic field to close the reed switch. The phase change pressure sensing concept was demonstrated in testing. However, the available equipment was unable to reach the pressures required to verify that propylene glycol will behave as expected. Further testing on a sounding rocket will be conducted by Sandia. Our testing also revealed flaws in the method used to fill and seal the reservoir diaphragm system. A more robust filling method was proposed in Chapter 5.

This project provided an early prototype of the vacuum sensor and showed functional concepts for detecting launch acceleration and using expansion based on pressure change to move a magnetic actuator and close a reed switch. The development of a superior filling and sealing method for the reservoir diaphragm system is recommended for future work. Also, specialized PCFs may be designed to vaporize in the desired pressure range. In this report we selected a viable fluid that was safe to handle and readily available. The base was 3D printed for quick manufacturing and opening the possibility of manufacturing complex geometries. This allows for future iterations of the base to be optimized to be structurally sound while reducing material cost, mass, and lead-time.

References

- Aerocon. (2017). *G Switches / Acceleration Switches*. Retrieved from Aerocon:
<http://www.aeroconsystems.com/electronics/switch-acceleration.htm>
- Cajori, F. (1929). *History of Determinations of the Heights of Mountains*. Retrieved from Isis, Volume 12 No. 3, pp. 482-514:
http://penelope.uchicago.edu/Thayer/E/Journals/ISIS/12/3/Determinations_of_Heights_of_Mountains*.html
- Center for Disease Control. (1997). *Public Health Statement for Propylene Glycol*. Retrieved from Center for Disease Control:
<https://www.atsdr.cdc.gov/phs/phs.asp?id=1120&tid=240>
- Chemical Engineering and Materials Research Information Center (CHERIC). (2018). *Pure Component Properties*. Retrieved from Chemical Engineering and Materials Research Information Center (CHERIC): <https://www.cheric.org/research/kdb/hcprop/cmprch.php>
- CP Lab Safety. (2018). *Aluminum Chemical Compatibility*. Retrieved from CP Lab Safety:
<https://www.calpaclab.com/aluminum-chemical-compatibility-chart/>
- Granta Design Limited. (2017). *CES EduPack software*. Retrieved from Granta Design Limited:
www.grantadesign.com
- Hillyard, N., & Cunningham, A. (1994). *Low Density Cellular Plastics Physical Basis of Behavior, 1st Edition*. Great Britain: Chapman and Hall.
- Huo, M., Chuai, R., Yin, L., Liu, X., & Wang, X. (2006). Self-testable Pressure Sensors Based on Phase Change. *1st IEEE International Conference on Nano/Micro Engineered and Molecular Systems*.
- K&J Magnetics. (n.d.). *Frequently Asked Questions*. Retrieved from K&J Magnetics:
<https://www.kjmagnetics.com/FAQ.asp#pulllift>
- K&J Magnetics. (n.d.). *R622CS Magnetic Pull Force Case 1*. Retrieved from K&J Magnetics:
<https://www.kjmagnetics.com/largergraph.asp?CI=1&pName=R622CS-P>

Lewis, B. (2007). *File Exchange: Complete 1976 Standard Atmosphere*. Retrieved from MathWorks: <https://www.mathworks.com/matlabcentral/fileexchange/13635-complete-1976-standard-atmosphere>

Littlefuse. (n.d.). *DRS-50 50.8mm High Power Reed Switch*. Retrieved from Littlefuse: http://www.littelfuse.com/~media/electronics/datasheets/reed_switches/littelfuse_reed_switch_drs-50_datasheet.pdf

Mathworks. (2018). *R2018a Documentation: Solve Stiff Problems*. Retrieved from Mathworks Help: <https://www.mathworks.com/help/matlab/math/solve-stiff-odes.html>

National Institute of Standards and Technology (NIST). (2017). *NIST Standard Reference Database Number 69*. Retrieved from NIST Chemistry WebBook: <https://webbook.nist.gov/chemistry/>

ThermoFischer Scientific. (n.d.). *Labware Chemical Resistance Table*. Retrieved from ThermoFischer Scientific: <https://tools.thermofisher.com/content/sfs/brochures/D20480~.pdf>

Appendices

Additional Figures

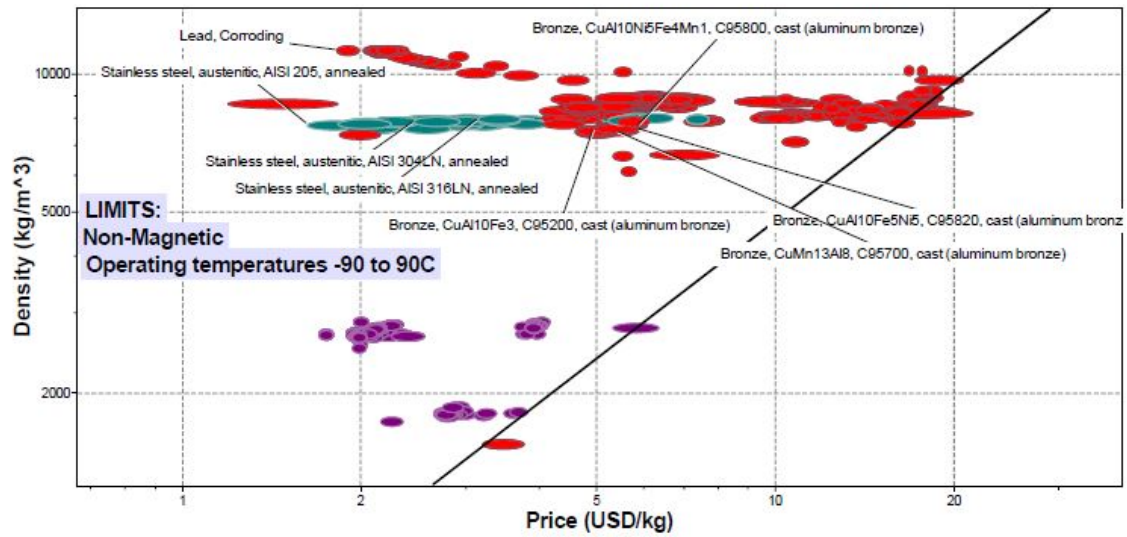


Figure 10: Density vs. Price per kg

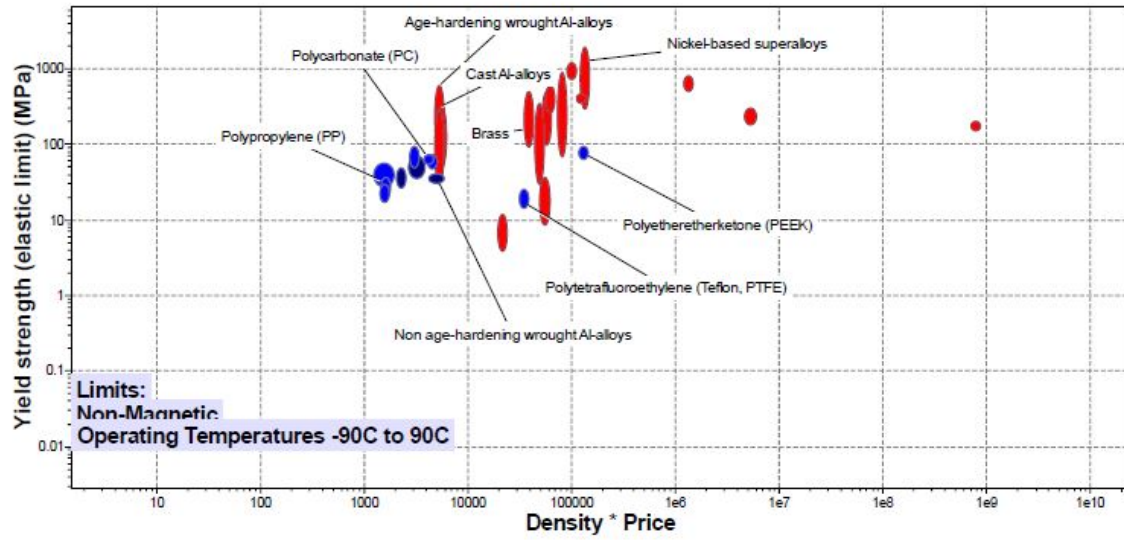


Figure 11: Strength vs Density * Price

Part Drawings

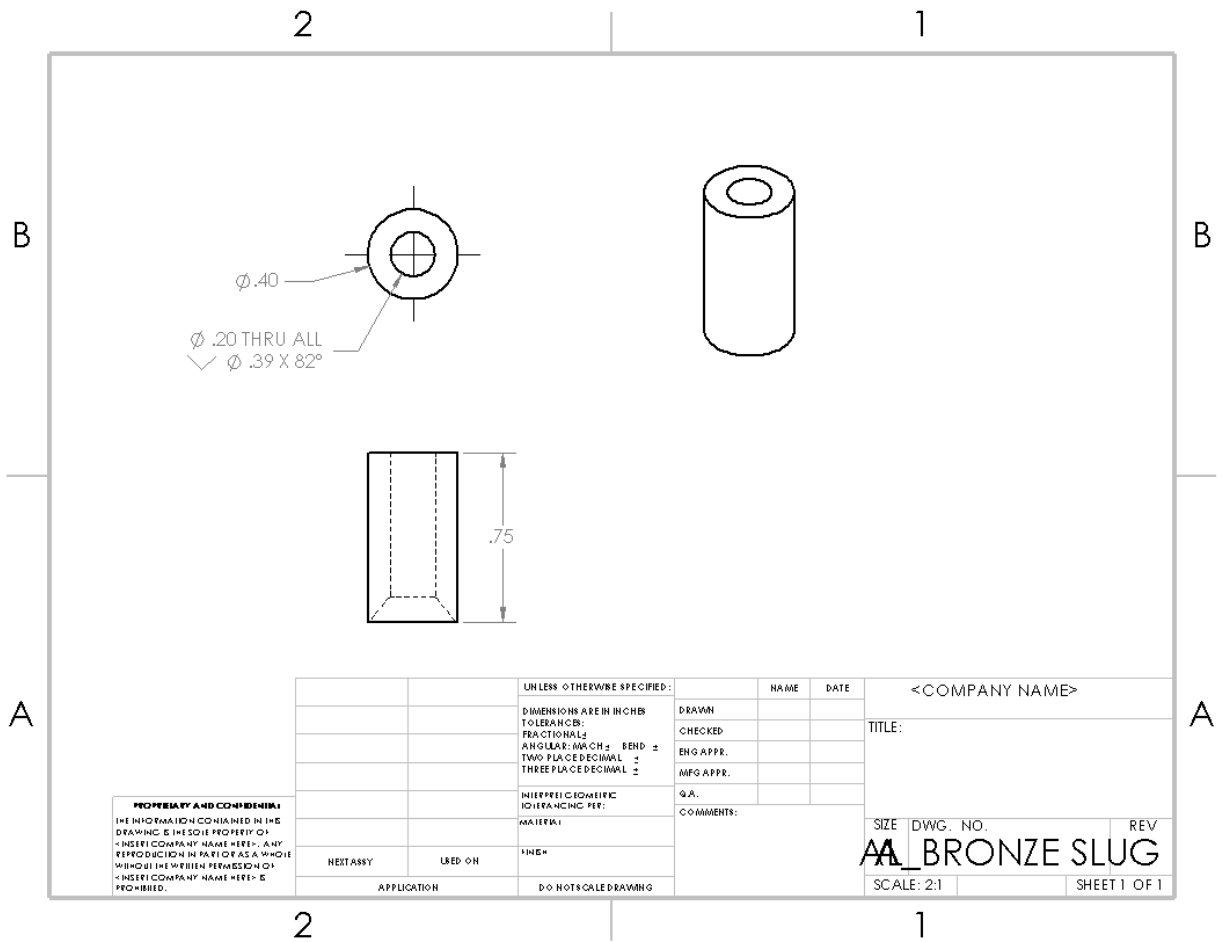


Figure 12: Al-Bronze slug Drawing

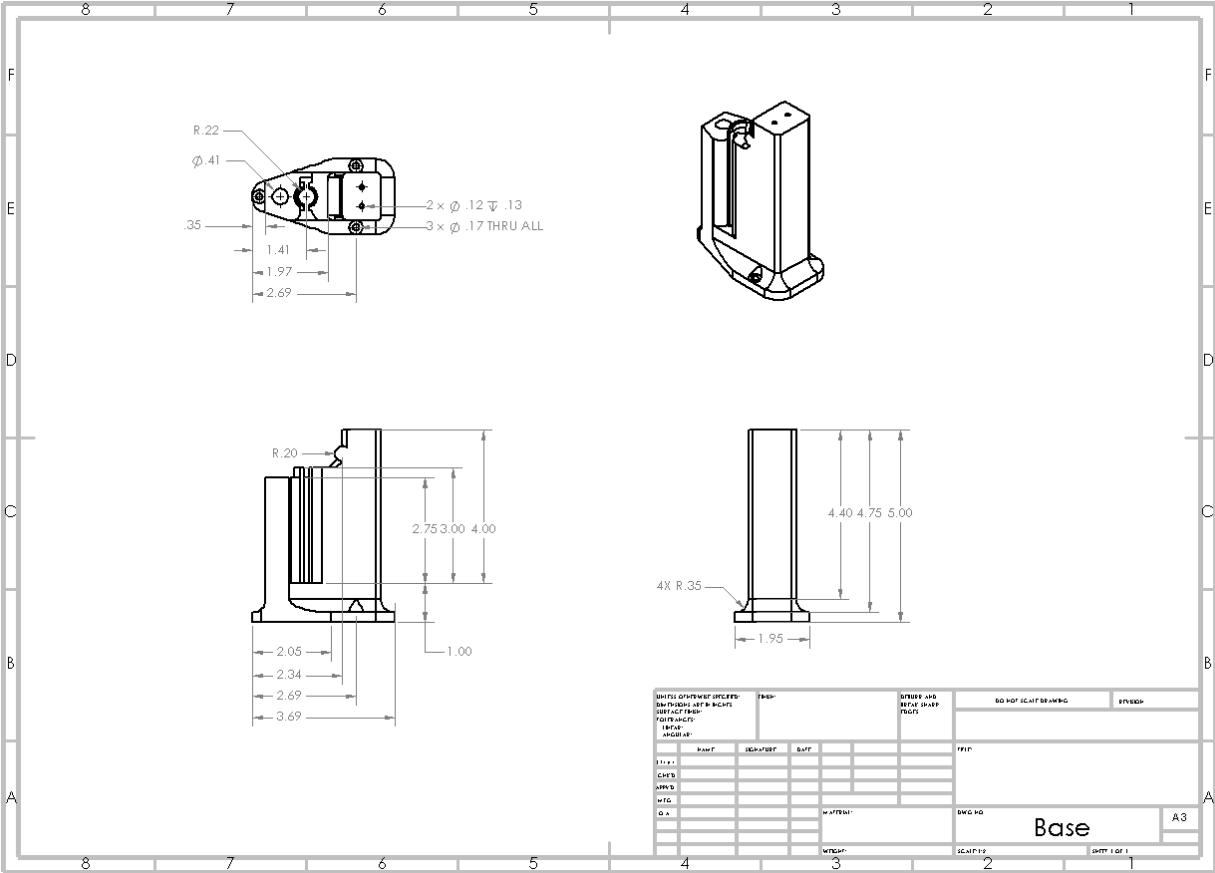


Figure 13: 3D printed base Drawing

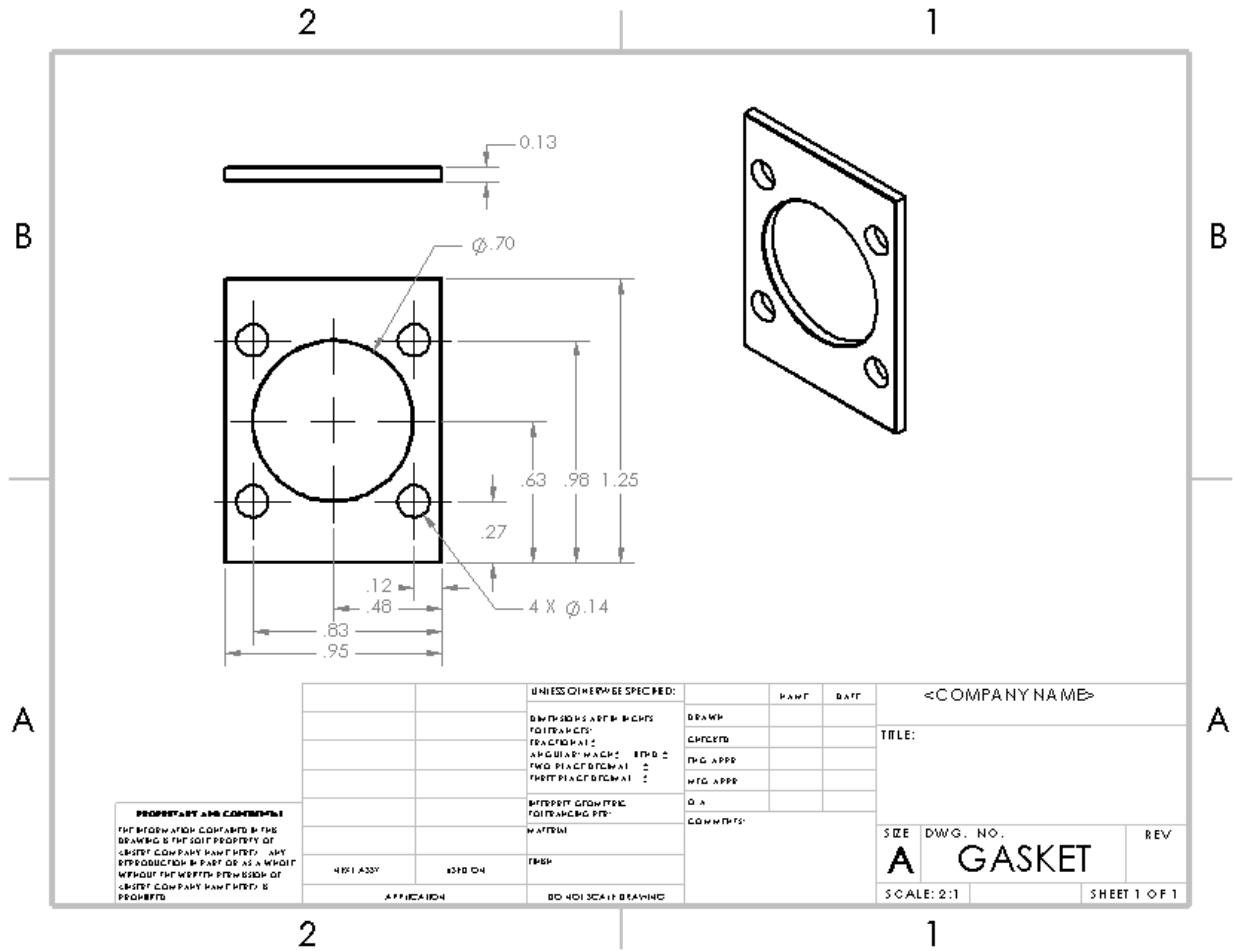


Figure 14: Expanded PTFE Gasket Drawing

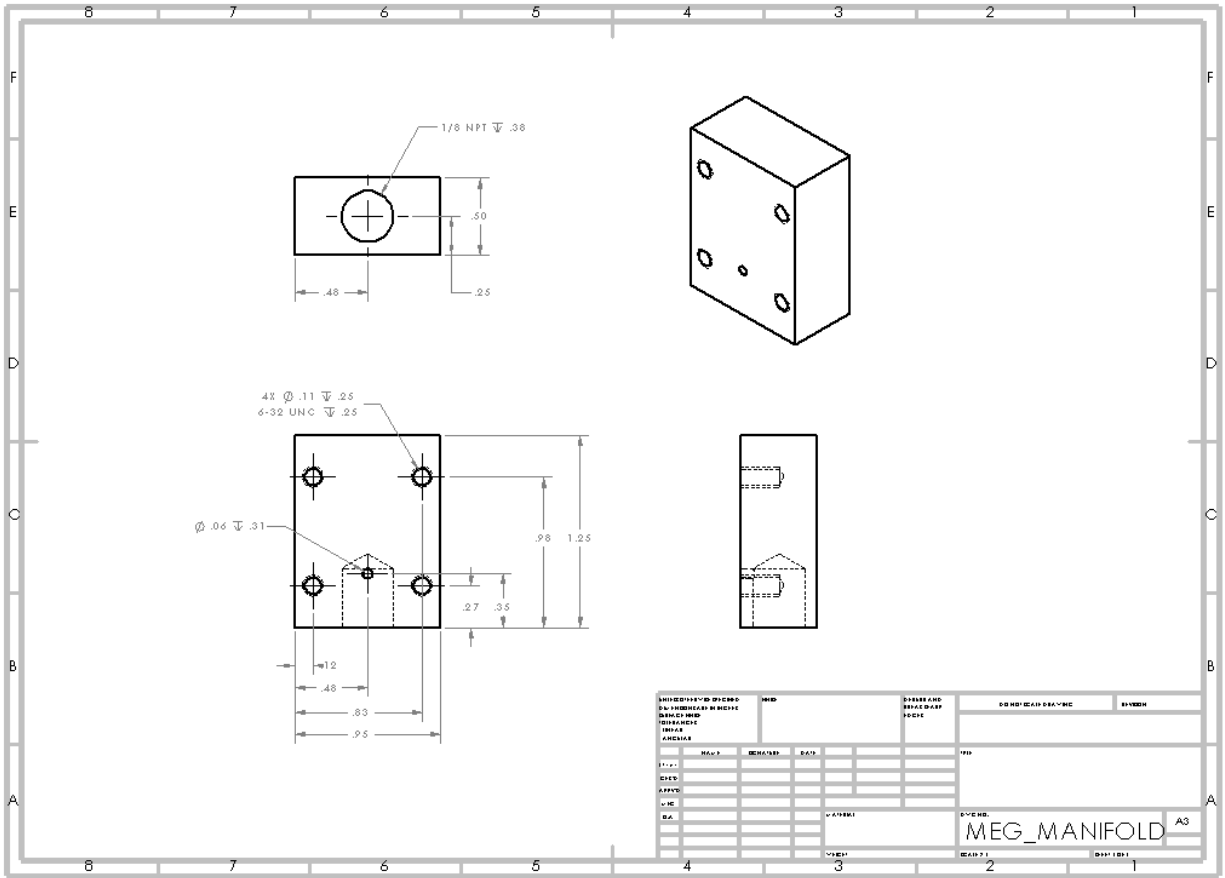


Figure 15: Pressure Sensor manifold Drawing

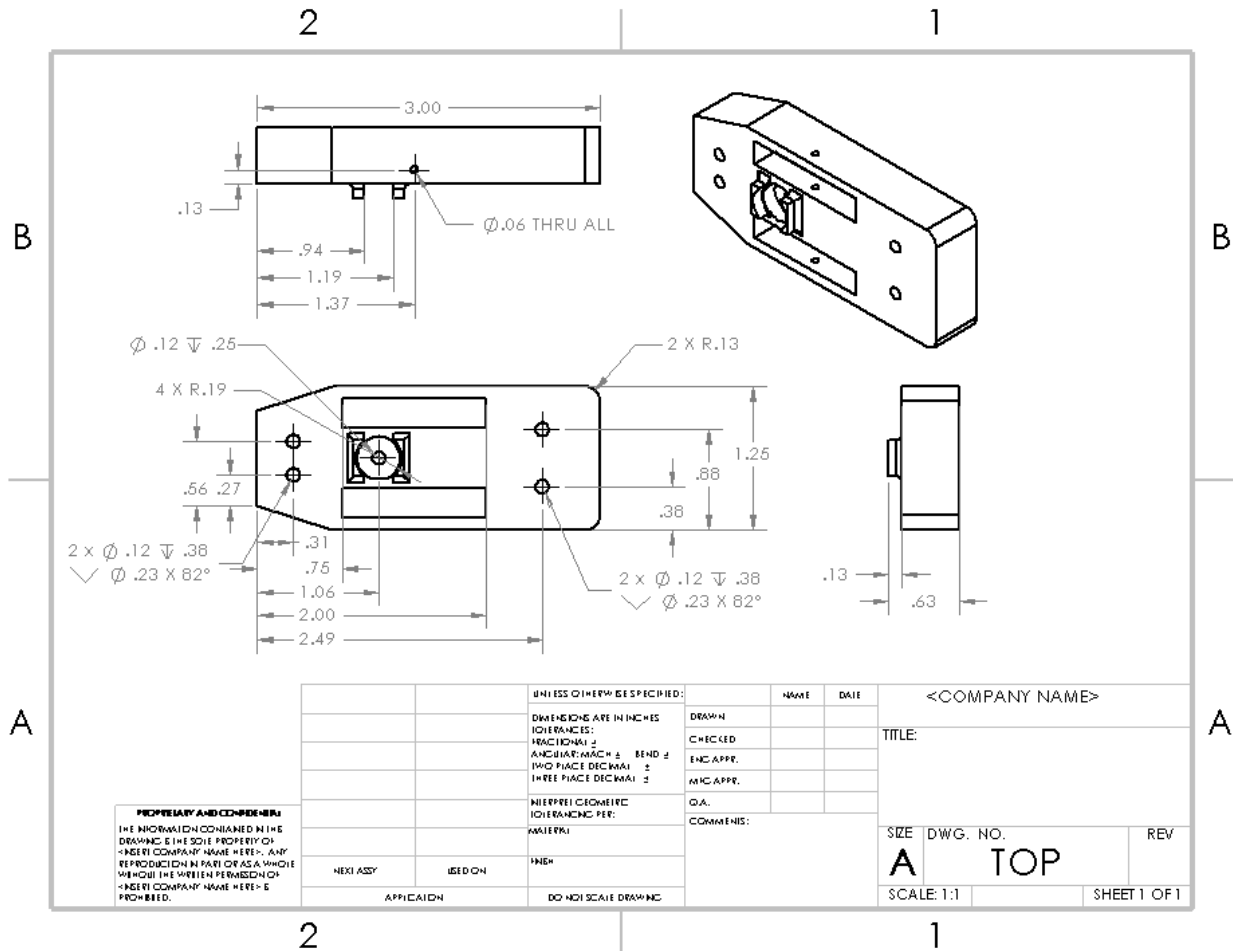


Figure 16: 3D printed top Drawing

Assembly Drawing

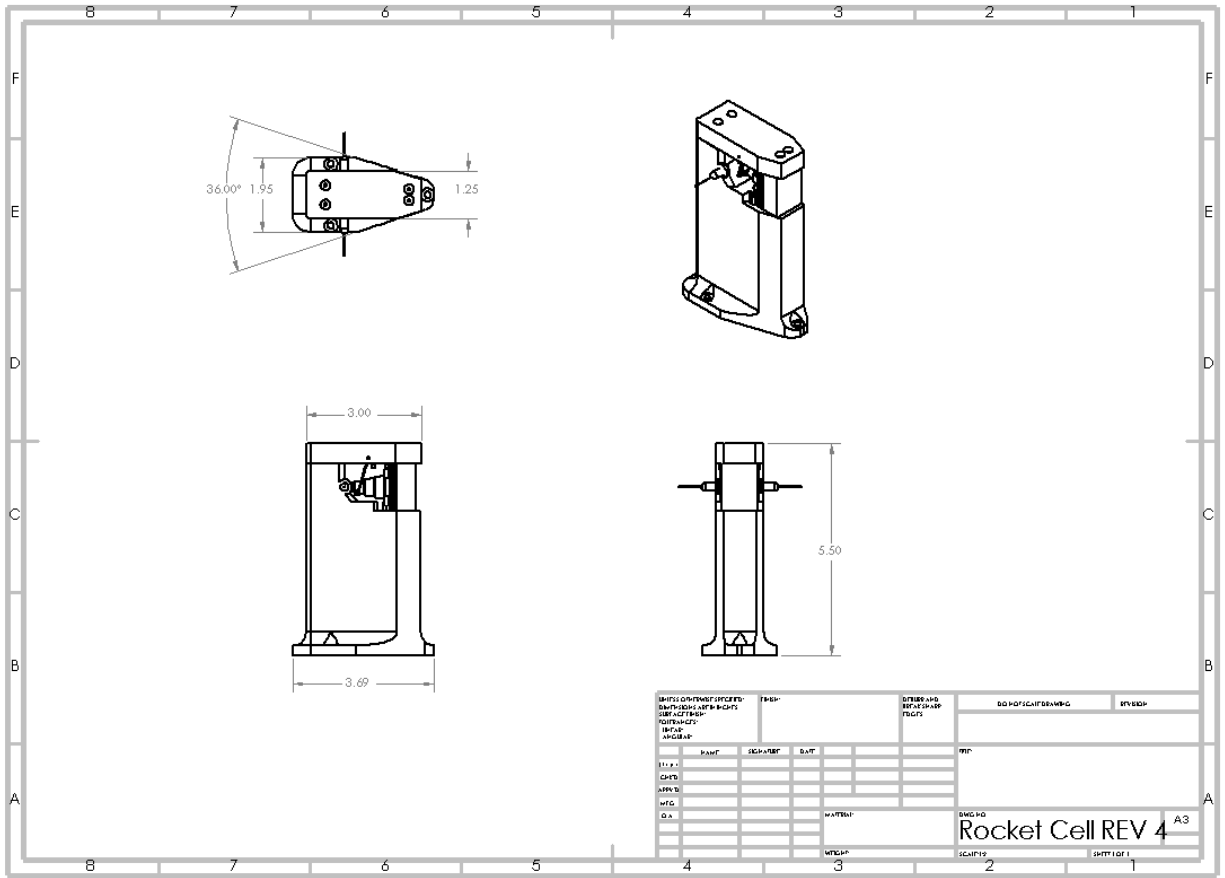


Figure 17: Assembly Drawing

Exploded View

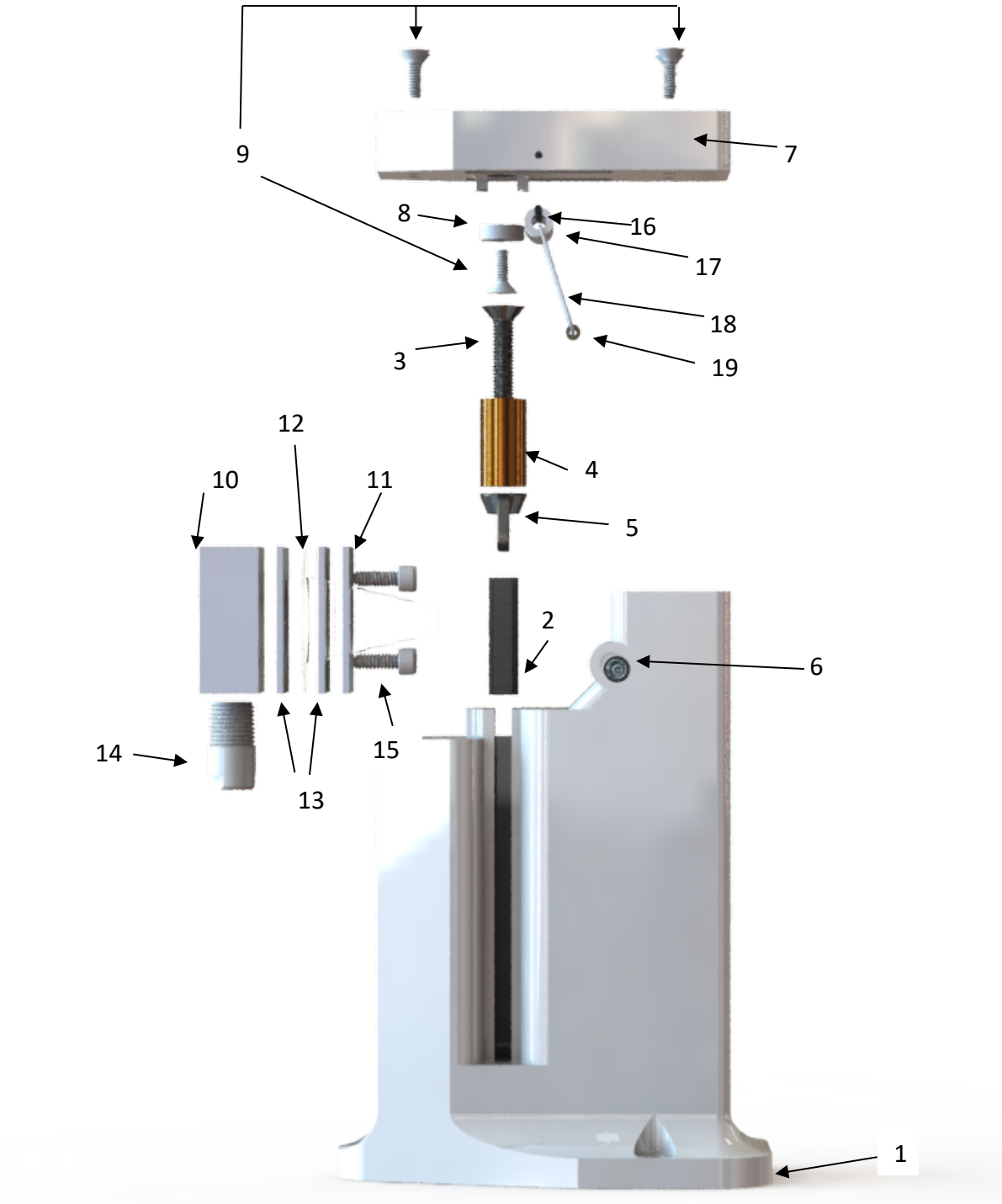


Figure 18: Exploded View Render

Table 6: Exploded View Component List

Component	Exploded View Label #
Base	1
Damping Foam	2
10-32 Steel Screw	3
10-32 Steel Wingnut	4
AL-Bronze Slug	5
Reed Switch	6
Base Top	7
#4 Countersunk Magnet	8
#4-40 Countersunk Screw	9
Manifold/Reservoir	10
Flange	11
FEP Diaphragm	12
PTFE Gasket	13
PTFE 1/8 NPT Plug	14
6-32 Cap Screw	15
Carbon Fiber Rod	16
PTFE Wire Sleeve	17
Wire Loop	18
N52 Ring Magnet (set of 5)	19

Matlab Scripts

sandia_model.m

```
%% Senior Design Dynamic Model
% Solution to dynamic model for acceleration switch
clear,clc
Fm = @(x) 0.942*exp(-238*(x+(0.00125))); % Magnet force curve fit [x= distance from magnet in feet]
ua_max = 19.6*32.2; % rocket acceleration [g]*[32.2ft/s/s]
m = .035/32.2; % [slug]
tspan=[0,3]; % Look between 0 and 0.1 seconds
y0=[0,0]; % initial conditions x(0)=0.015in from magnet surface, x'(0)=0ft/s
sol = ode15s(@(t,y) accel_odefcn(t,y,m*ua_max,m,Fm), tspan, y0); % Use stiff Solver
t=sol.x;
y=sol.y';
% Mathworks claims ode15s performs best for most stiff problems.
LOI=find(y(:,1)>0.25);% Find first index where x > 3 inches
LOI2=find(y(:,1)<0.25);% Find lastt index where x < 3 inches
if length(LOI) <2 % For accelerations where switch does not trip
    LOI=length(y);
    V=0;
    t_I=0;
    x_I = 0;
else
    LOI=LOI(1);
    LOI2=LOI2(end);
    %linear interpolation to find time where x=3 inch
    t_I = t(LOI2)+(t(LOI2)-t(LOI))*((0.25-y(LOI2,1))/(y(LOI2,1)-y(LOI2,1)));
    v_loi1 = find(t<t_I);
    v_loi1=v_loi1(end);
    v_loi2 = find(t>t_I);
    v_loi2=v_loi2(1);
    % Linear interpolation to find velocity at time t_I ( when x=3 inch)
    V = y(v_loi1,2) + (y(v_loi2,2)-y(v_loi1,2))*((t_I-t(v_loi1))/(t(v_loi2)-t(v_loi1)));
    disp('Velocity at x=3in is')
    disp(strcat(num2str(V),'ft/s.))
    disp('This occurs at')
    disp(strcat('t=',num2str(t_I),'seconds.))
    x_I = 0.25; %x =3 inch
end
figure(1)
plot(t(1:LOI),y(1:LOI,1),'b') % plot position (ft) vs time
title('X Position vs Time')
xlabel('Time(s)')
ylabel('Position (ft)')
hold on
plot([t_I,t_I],[0,x_I],'r--')
plot([0,t_I],[x_I,x_I],'r--')
hold off
figure(2)
plot(t(1:LOI),y(1:LOI,2),'b') % plot velocity(ft/s) vs time
```

```

title('X Velocity vs Time')
xlabel('Time(s)')
ylabel('Velocity (ft/s)')
hold on
plot([t_I,t_I],[0,V],'r--')
plot([0,t_I],[V,V],'r--')
hold off

```

accel_odefcn.m

```

function dydt = accel_odefcn(t,y,a_max,m,Fm)
% System of first order ODEs made from 2nd order ODE
%  $mx'' + Fm(x) - Fc(x) = \mu$ 
dydt = zeros(2,1);
dydt(1) = y(2);
dydt(2) = ((a_max)-Fm(y(1))+contact_force(y(1),m,a_max,Fm))/m;

```

contact_force.m

```

function val = contact_force(x,m,a_max,Fm)
% Contact force required before the magnet and mass separate.
%  $F_c = F_m(0) - m \cdot a_{\text{rocket}}$ 
val=zeros(length(x),1);
z=1e-6;
for i=1:length(x)
if x(i)<=z
v=(Fm(0)-(m*a_max));
% For small x, contact force behave as stiff spring
val(i)=((-v/z).*(x(i)))+v;
else
val(i)=0;
end
end
end

```

vapor_press.m

```

% Vapor Pressures
%
clear
%
%% Set Temperature Range
%
t = linspace(-100,400,1000); % -100°C to 400°C (Careful! Extrapolating data on the ends)
%
% Import the vapor pressure curves for various liquids
% Ethylene Glycol https://www.thermo.com/research/kdb/hcprop/showprop.php?cmpid=909
% Propylene Glycol https://www.thermo.com/research/kdb/hcprop/showcoef.php?cmpid=910&prop=PVP
% Hexane https://www.thermo.com/research/kdb/hcprop/showcoef.php?cmpid=6&prop=PVP

```

```

% Isopropanol https://www.thermo.com/research/kdb/hcprop/showcoef.php?cmpid=820&prop=PVP
name = {'Ethylene Glycol [-10 to 371 °C]', 'Propylene Glycol [-60 to 353 °C ]', 'Hexane [-95 to 234°C]...',
'Diethylene Glycol [-11 to 471°C]', 'Isopropanol [-88 235°C]'};
lgth = length(name); % To retrieve number of compounds assessed

a = [-2.599771e1 -3.084306e1 -1.399935E+01 -1.283727E+01 -7.694051E+00];
b = [-1.476857e4 -1.609752e4 -7.284572E+03 -1.285564E+04 -7.690896E+03];
c = [ 1.914250e2 2.235649e2 1.059605E+02 1.087915E+02 7.134113E+01];
d = [ 2.062331e-5 2.420669e-5 1.410325E-05 3.169949E-06 7.656355E-07];

pv = zeros(1000,lgth);

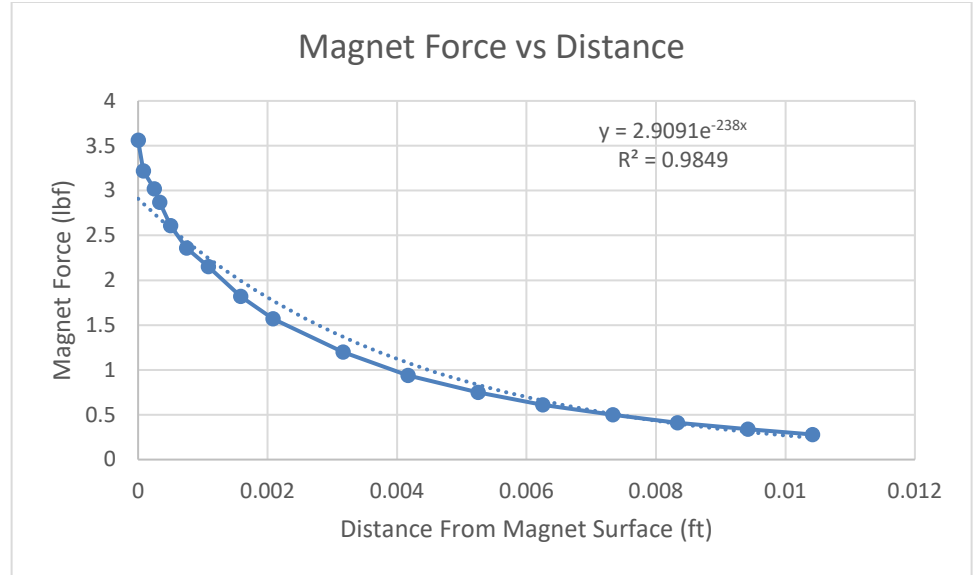
for i= 1:lgth
    pv(:,i) = exp( log(760/101.335) + a(i).*log(t+273.15) + (b(i)./(t+273.15)) +c(i) + d(i).*(t+273.15).^2);
end
%
%
%% Get Standard Atmosphere Data for high altitudes
%
%
[Z Z_L Z_U T P rho c g mu nu k n n_sum] = atmo;
% Filter Data
index = find(P < 13 & P > 13e-5); % Only keep switch pressure range
length = length(index);
Z = Z( index(1) : index(length)); % Get altitude where we see the switch pressure range
P = P( index(1) : index(length))/133.3224; % get the pressure data within the range and convert to mmHg
T = T( index(1) : index(length)) - 273.15; % Get the corresponding temperatures within the range, convert to °C
%
%% Plots
%
%
for i = 1:lgth
    figure(i)
    semilogy(t,pv(:,i),'LineWidth',2)
    grid on
    hold on
    semilogy([-100,600],[10^-1,10^-1],'r');
    hold on
    semilogy([-100,600],[10^-6,10^-6],'r');
    hold on
    semilogy(T,P,'k', 'LineWidth', 2)
    %semilogy(T,P,'-s','MarkerFaceColor',[.8 .8 .8])
    title(name(i),'FontSize',14);
    xlabel('Temperature (C°)','FontSize',14);
    ylabel('Vapor Pressure (mmHg)','FontSize',14);
end

```

Magnet Data from K&J Magnetics With Curve Fit

d (in)	d(ft)	F (lbf)
0	0	3.56
0.001	8.33E-05	3.22
0.003	0.00025	3.02

0.004	0.000333	2.87
0.006	0.0005	2.61
0.009	0.00075	2.36
0.013	0.001083	2.15
0.019	0.001583	1.82
0.025	0.002083	1.57
0.038	0.003167	1.2
0.05	0.004167	0.94
0.063	0.00525	0.75
0.075	0.00625	0.61
0.088	0.007333	0.5
0.1	0.008333	0.41
0.113	0.009417	0.34
0.125	0.010417	0.28



Scale Factor = 0.324

(Actual/K&J Data)

Scaled Curve Fit: $F_m = 0.942e^{-238x}$, where x is in ft.

Vapor Pressure Plots

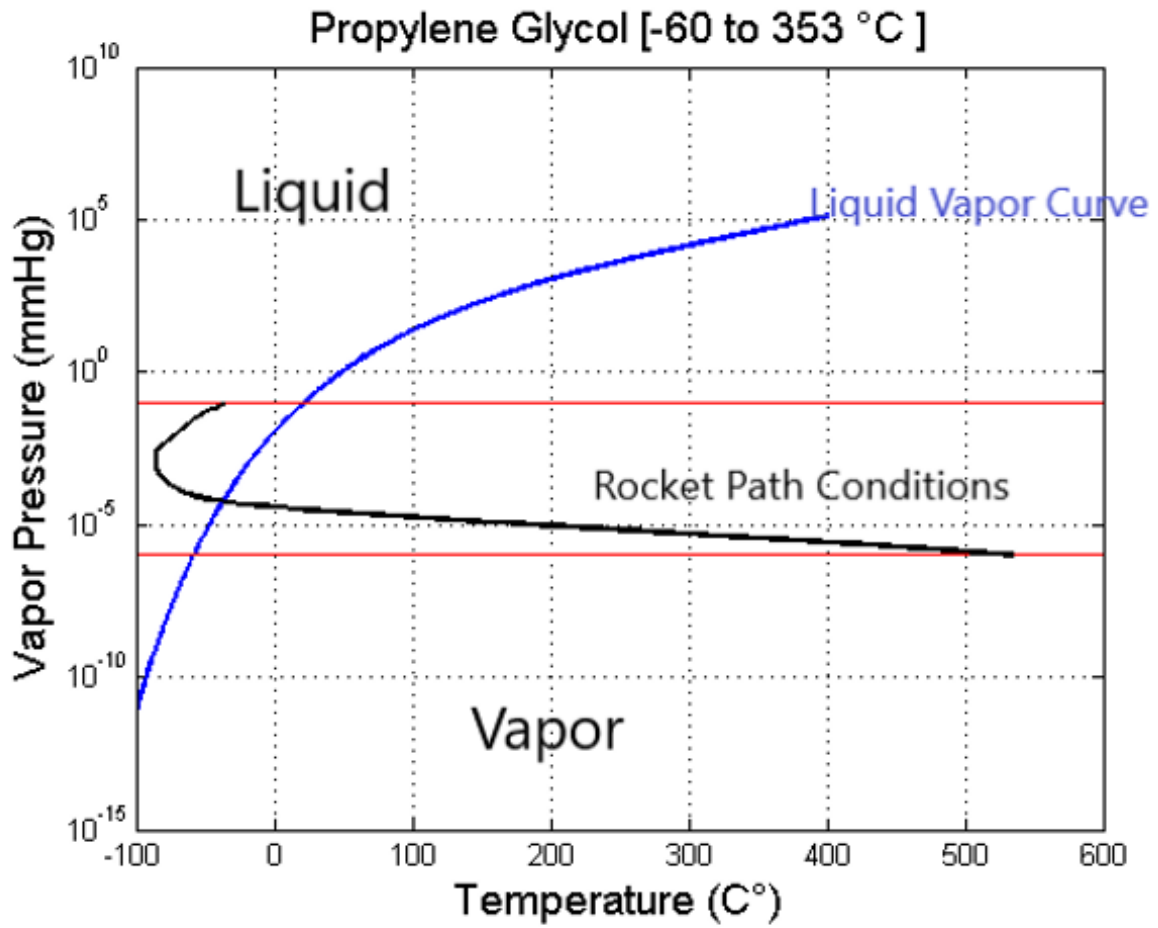


Figure 19: Vapor Pressure Plots

Additional Concept Drawings

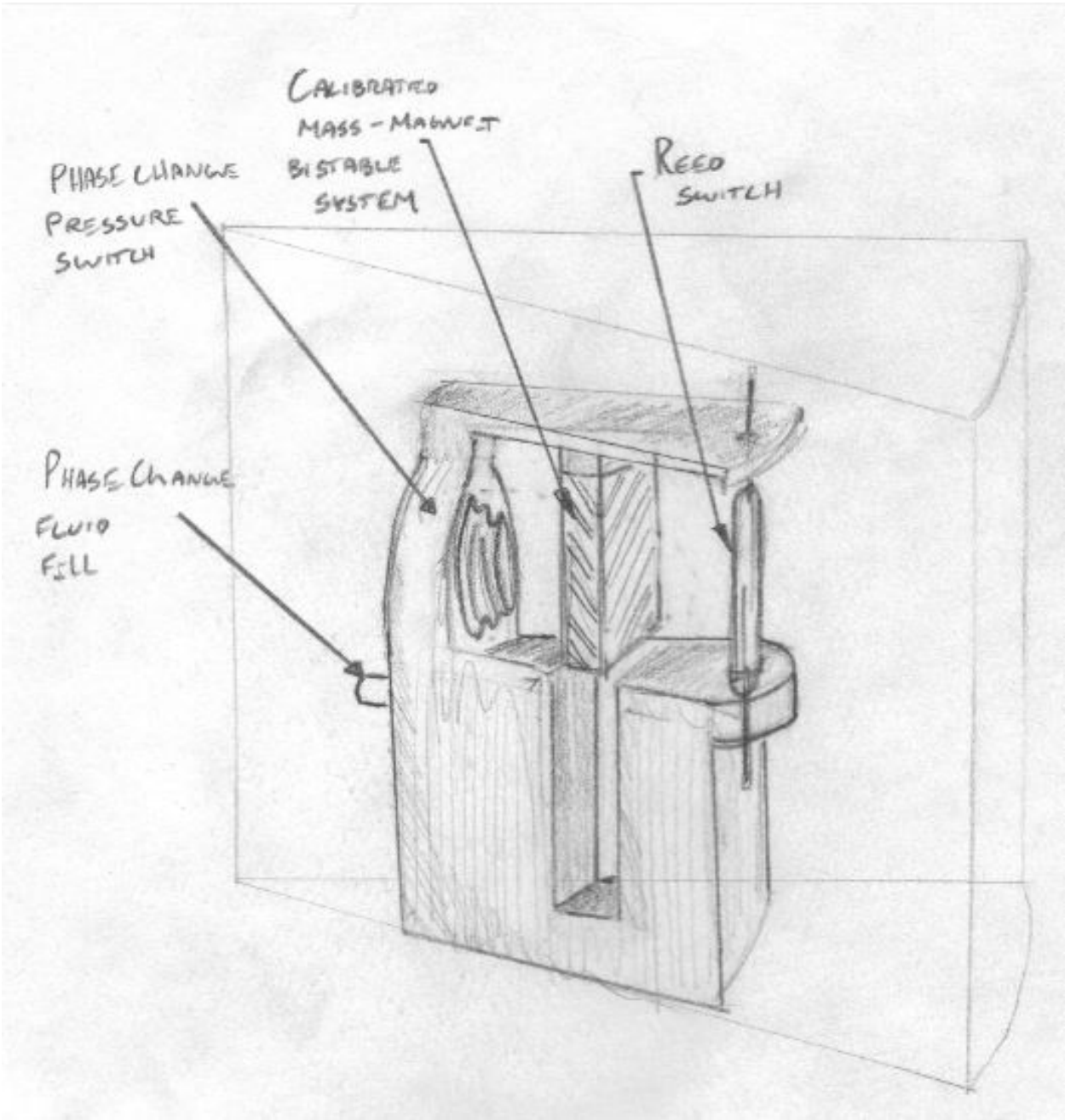


Figure 20: 3D Concept Drawing

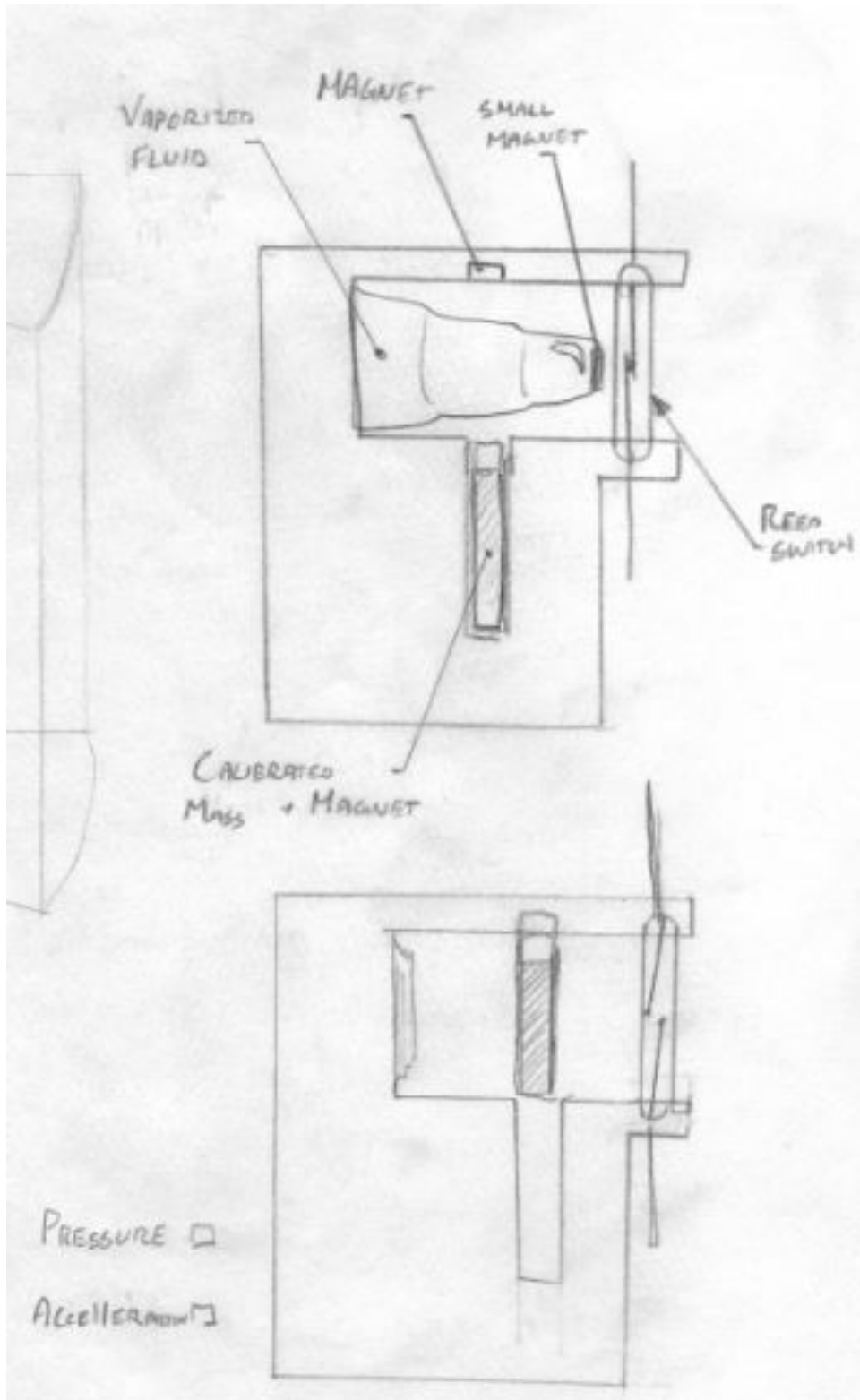


Figure 21: Set and Unset Positions